

¹ Supplementary information for: Cropland abandonment is largely
² fleeting, limiting its potential environmental benefits

³ Christopher L. Crawford^{1*} He Yin² Volker C. Radeloff³ David S. Wilcove^{1,4}

⁴ ¹Princeton School of Public and International Affairs, Princeton University, Princeton, NJ

⁵ ²Department of Geography, Kent State University, Kent, OH

⁶ ³SILVIS Lab, Department of Forest & Wildlife Ecology, University of Wisconsin - Madison,
⁷ Madison, WI

⁸ ⁴Department of Ecology & Evolutionary Biology, Princeton University, Princeton, NJ

⁹ September 16, 2021

¹¹ **Contents**

¹² S1 Extended Results	⁵
¹³ S1.1 Limited abandonment in Mato Grosso	⁵
¹⁴ S1.2 Biomes	⁵
¹⁵ S1.3 The effect of varying abandonment definitions	⁶
¹⁶ S1.4 Comparing annual and two-year estimates of abandonment	⁶
¹⁷ S1.5 Maps of abandonment duration as of 2017 and maximum duration during time series	⁶
¹⁸ S2 Extended Methods	⁷
¹⁹ S2.1 Classifying abandonment	⁷
²⁰ S2.2 Temporal filters	⁷
²¹ S2.3 Modeling abandonment decay	⁷
²² S2.4 Change in recultivation rates over time	⁹
²³ S2.5 Projecting abandonment duration into the future	⁹
²⁴ References	¹⁰
²⁵ S3 Supplementary Tables	¹¹
²⁶ S4 Supplementary Figures	¹²

*Corresponding Author, ccrawford@princeton.edu, Robertson Hall, Princeton University, Princeton, NJ

27 **List of Tables**

28	S1	Summary statistics describing the duration of abandonment (in years) at our eleven sites 29 between 1987 and 2017, using a five year abandonment definition, and incorporating all periods 30 of abandonment (allowing for multiple per pixel).	11
31	S2	Cropland abandonment (in Mha) as of 2017 as identified using a) our annual time series and a 32 five-year abandonment definition and b) a two year method taking the difference between land 33 cover in 1987 and 2017.	11

34 **List of Figures**

35	S1	The locations of our 11 sites, from Yin et al. ⁶ Sites are labeled as follows: (b) Vitebsk, Belarus 36 / Smolensk, Russia; (bh) Bosnia & Herzegovina; (c) Chongqing, China; (g) Goiás, Brazil; (i) 37 Iraq; (mg) Mato Grosso, Brazil; (n) Nebraska/Wyoming, USA; (o) Orenburg, Russia / Uralsk, 38 Kazakhstan; (s) Shaanxi/Shanxi, China; (v) Volgograd, Russia; (w) Wisconsin, USA.	12
39	S2	Area abandoned a) as of 2017, b) at any point between 1987-2017, c) as of 2017 as a proportion 40 of the total cropland extent (i.e., the area of all lands that were cultivated at some point during 41 the time series). Note that sites are shown in ascending order of area abandoned as of 2017 as 42 a proportion of total cropland extent.	13
43	S3	Cumulative area abandoned at each site through time, according to age class (in years).	14
44	S4	Area in each land cover class at each site through time. Land cover classes are cropland, 45 grassland, woody vegetation, non-vegetation, and abandoned (for at least 5 years).	15
46	S5	Annual turnover of abandoned croplands at each site, showing the annual gain (dark green) 47 and annual loss (i.e., recultivation, light green) and net change (black line) of abandoned 48 croplands.	16
49	S6	The distribution of the maximum abandonment duration (in years) for each pixel at each 50 site from 1987 to 2017. The y-scale shows the proportion of pixels with maximum duration 51 values of a given duration at each site. As previously noted, abandonment and recultivation 52 can occur multiple times at a single pixel during our time series, and this figure serves as a 53 companion to the distribution of all abandonment values shown in Figure 2. Site-level mean 54 duration values are shown in the red and blue dots, corresponding to mean values calculated 55 across all periods of abandonment (in red, including multiple periods per pixel) and mean 56 values calculated across only the maximum duration of abandonment at each pixel (in blue). 57 The vertical dashed lines represent the mean of these site-level mean duration values, for all 58 abandonment periods (red) and only the maximum duration at each pixel (blue), respectively.	17
59	S7	Maximum duration of cropland abandonment (in years) observed at each pixel between 1987 60 and 2017 in our eleven study sites. This serves as a companion to maps of the abandonment 61 duration as of 2017 shown in Figure 1. Site locations are shown in Figure S1.	18
62	S8	Proportion of abandoned cropland in each land cover class as of 2017.	19
63	S9	Site biomes, using biome classifications from The Nature Conservancy's Terrestrial Ecoregions 64 of The World (TEOW) database, derived from Olson et al. ¹² and Olson and Dinerstein. ¹³ . .	20
65	S10	Mean abandonment lengths shown for various abandonment thresholds.	21
66	S11	Recultivation rates shown for various abandonment thresholds.	22

67	S12 Decay model results for all sites, showing the proportion of each cohort of abandoned land (i.e., all pixels abandoned in a given year) remaining abandoned over time for each of our eleven sites. Points represent actual observations by cohort, dashed lines represent linear model predictions (fitted values) for each cohort as a function of time (including a linear and logarithmic term of time), and the solid black line represents the site-level mean trend across all cohorts (calculated by taking the mean of each time coefficient values across all cohorts, respectively, and using those two mean values to plot a mean trend). Colors of both points and dashed lines correspond to roughly five-year group of cohorts, ranging from dark purple (oldest cohorts) to green and yellow (most recent cohorts). The horizontal black dashed line shows a proportion of 0.5, indicating the point where half of a cohort has been recultivated. Model diagnostic plots are shown in Figures S14 and S15.	23
78	S13 Akaike Information Criterion (AIC) values for various recultivation (“decay”) model specifica- tions for each site. More negative AIC values indicate a better model fit.	24
80	S14 Residuals vs. fitted diagnostic plots for our linear models of the recultivation (“decay”) of abandonment at each site. These models take the form shown in Equation (S2), and are shown in Figure S12.	25
83	S15 QQ plots calculated using the <code>{car}</code> package ¹⁴ for our linear models of the recultivation (“decay”) of abandonment at each site. These models take the form shown in Equation (S2), and are shown in Figure S12.	26
86	S16 Mean decay model coefficients across cohorts at each site. The left panel shows the mean coefficient on the log(time) terms and the right shows the site mean coefficient on the linear time terms. These mean coefficients are used to plot the mean decay trajectories shown in Figure 3.	27
90	S17 An alternative representation of the mean decay rate for each site (also shown in Figure 3). The color of each point corresponds to the proportion remaining after a given amount of time.	28
92	S18 The rate of change of decay rates (measured as the half-life, or the time required for 50% of each cohort to be recultivated) at each site over the course of the time series. Individual site trends are shown in panel a. Solid lines show simple linear regressions, the slopes of which are shown in panel b. Gray bands around the linear trends in panel a and the error bars on slope estimates in panel b both represent 95% confidence intervals. These models are described by Eq. (S3). Model diagnostic plots are shown in Figures S19 and S20.	29
98	S19 Residuals vs. fitted diagnostic plots for each site, for a simple <code>lm</code> call corresponding to Eq. (S3), in which the half-life (i.e., the time required for half (50%) of a given cohort of abandoned cropland to be recultivated) is modeled as a function of the year of initial abandonment at each site.	30
102	S20 QQ plots calculated using the <code>car</code> package ⁽¹⁴⁾ , for a simple <code>lm</code> call corresponding to Eq. (S3), in which the half-life (i.e., the time required for half (50%) of a given cohort of abandoned cropland to be recultivated) is modeled as a function of the year of initial abandonment at each site.	31
106	S21 Annual gain in newly abandoned cropland at our eleven sites. Panel a shows the trend in annual abandonment over time at each site (in 10^3 ha), and Panel b shows the mean annual abandonment (in 10^3 ha) at each site. The mean values in panel b feed into the extrapolations. Note that the annual gain in abandonment corresponds to the dark green bars in Figure S5.	32
110	S22 The results of our simple extrapolation, including a) the mean age of abandonment, and b) the total area abandoned into the future. Colors corresponding to each site are consistent across the three panels. These extrapolation assume recultivation based on the mean decay trend for each site Figure 3 and annual new abandonment based on the mean annual gain in abandonment shown in Figure S5 (dark green bars).	32

115	S23 Extrapolating area by age bin, assuming a 1) each site follows the mean recultivation (“decay”) 116 rate, and 2) a constant area abandoned each year (based on the mean annual area abandoned 117 at each site).	33
118	S24 The results of our second extrapolation, including a) the mean age of abandonment, and b) 119 the total area abandoned into the future. Colors corresponding to each site are consistent 120 across the three panels. These extrapolation assume recultivation based on the mean decay 121 trend for each site Figure 3 and annual new abandonment based on the mean annual gain in 122 abandonment shown in Figure S5 (dark green bars).	34
123	S25 Extrapolating area by age bin, assuming a 1) each site follows the mean recultivation (“decay”) 124 rate, and 2) a constant area abandoned each year until 2017 (based on the mean annual 125 area abandoned at each site), followed by a linearly declining area abandoned each year until 126 reaching 0 in 2050.	35
127	S26 Comparing the mean duration of abandonment at our 11 sites observed between 1987 and 128 2017 with the extrapolated mean duration as of 2050 for our two extrapolations.	36
129	S27 Abandonment patterns for Vitebsk, Belarus / Smolensk, Russia, showing a) accumulation of 130 abandoned land by age class, b) decay of abandoned land by year abandoned, c) the area in 131 each land cover class through time (including both land that has been abandoned for five or 132 more years, as well as any land abandoned for 1 or more years, therefore including short-term 133 fallows), d) the annual turnover of abandoned land through time, and e) the distribution 134 of abandonment duration for all periods of cropland abandonment (top) and the maximum 135 duration of abandonment at each pixel (bottom).	37
136	S28 Abandonment patterns for Bosnia & Herzegovina, following Figure S27.	38
137	S29 Abandonment patterns for Chongqing, China, following Figure S27.	39
138	S30 Abandonment patterns for Goiás, Brazil, following Figure S27.	40
139	S31 Abandonment patterns for Iraq, following Figure S27.	41
140	S32 Abandonment patterns for Mato Grosso, Brazil, following Figure S27.	42
141	S33 Abandonment patterns for Nebraska/Wyoming, USA, following Figure S27.	43
142	S34 Abandonment patterns for Orenburg, Russia / Uralsk, Kazakhstan, following Figure S27. . .	44
143	S35 Abandonment patterns for Shaanxi/Shanxi, China, following Figure S27.	45
144	S36 Abandonment patterns for Volgograd, Russia, following Figure S27.	46
145	S37 Abandonment patterns for Wisconsin, USA, following Figure S27.	47

¹⁴⁶ S1 Extended Results

¹⁴⁷ Cropland abandonment at individual sites (excluding Mato Grosso, see Section S1.A.) ranged between
¹⁴⁸ 314,374.8 ha (Shaanxi) and 930,424 ha (Orenburg) as of 2017 (Figure S3), and because our sites varied in
¹⁴⁹ size, this corresponded to between 7.91% (Nebraska) and 19.91% (Shaanxi) of the total area of each site
¹⁵⁰ (Figure S2).

¹⁵¹ On average, we found that cropland abandonment lasted for only 14.42 years ($SD = 1.52$ years) across our
¹⁵² time series at our eleven sites. Note, however, that these summary statistics are calculated based on the
¹⁵³ mean abandonment duration at each site, to account for different site sizes. The summary statistics reported
¹⁵⁴ are therefore the mean of the mean abandonment duration at each of our eleven sites, and the standard
¹⁵⁵ deviation of the mean abandonment duration at each of our eleven sites.

¹⁵⁶ We also calculated the mean standard deviation of abandonment duration across our sites, which was 7.78
¹⁵⁷ years. The former is a measure of the spread of mean abandonment lengths across the 11 sites, whereas the
¹⁵⁸ latter is a measure of the average spread of abandonment lengths at each site. See Table S1.

¹⁵⁹ The area abandoned at each site is shown in Figure S2 (see also Table S2). The area abandoned at each site,
¹⁶⁰ by age class, is shown in Figure S3, and the area in each land cover class at each site is shown in Figure S4.
¹⁶¹ Figure S3 shows that the timing of abandonment varied across sites; some sites showed more abandonment
¹⁶² earlier in the time series (e.g., Iraq; Bosnia & Herzegovina; Volgograd, Russia; Nebraska/Wyoming, USA;
¹⁶³ & Mato Grosso, Brazil), some showed consistent abandonment over time (e.g., Vitebsk, Belarus/Smolensk,
¹⁶⁴ Russia; Goiás, Brazil; and Wisconsin, USA), and others showed increasing abandonment later on in the time
¹⁶⁵ series (e.g., sites in Shaanxi/Shanxi and Chongqing, China). Furthermore, Figure S5 shows the annual gain,
¹⁶⁶ loss, and net change in the area of abandoned croplands abandoned at each site.

¹⁶⁷ S1.1 Limited abandonment in Mato Grosso

¹⁶⁸ Mato Grosso, Brazil, was the only site that did not experience significant amounts of cropland abandonment
¹⁶⁹ during our time series. This is unsurprising given the recent history of agriculturally-driven land-use change
¹⁷⁰ over the last few decades. That being said, the abandonment that did take place in Mato Grosso was relatively
¹⁷¹ more durable, requiring 25 years to decline by half and 110 years for complete turnover. However, because
¹⁷² Mato Grosso showed large amounts of new cultivation over the source of our time series and relatively little
¹⁷³ abandonment (9,006 ha, or 0.47% of the total cropland extent, as of 2017), these results should be interpreted
¹⁷⁴ with care.

¹⁷⁵ S1.2 Biomes

¹⁷⁶ Some ecosystems and biomes seem to recover more quickly than others, namely in relatively higher latitudes,
¹⁷⁷ relatively colder climates, and in relatively more humid biomes.¹ Our sites cover a range of biomes (Figure
¹⁷⁸ S9), including:

- ¹⁷⁹ • Temperate Broadleaf and Mixed Forests (Vitebsk Belarus/Smolensk, Russia; Bosnia & Herzegovina;
¹⁸⁰ Wisconsin, USA),
- ¹⁸¹ • Temperate Grasslands, Savannas, and Shrublands (Nebraska/Wyoming, USA; Orenburg, Russia/Uralsk,
¹⁸² Kazakhstan; Volgograd, Russia),
- ¹⁸³ • Tropical Grassland (Goiás and Mato Grosso, Brazil),
- ¹⁸⁴ • Tropical Moist Broadleaf Forests (Chongqing, China; Mato Grosso, Brazil),
- ¹⁸⁵ • Montane Grassland and Shrublands (Shaanxi/Shanxi, China), and
- ¹⁸⁶ • Deserts & Xeric Shrublands (Iraq).

¹⁸⁷ The long-term land-cover outcomes for abandoned croplands are shown (as of 2017) in Figure S8. Land cover
¹⁸⁸ outcomes for abandoned croplands showed wide variation across sites, with most abandonment in Wisconsin

189 being classified as forest by 2017 (60% forest, 40% grassland), but remaining mostly in grassland elsewhere
190 (Figure S8). This limited woody vegetation regrowth may be a product of the biome, but it may simply be a
191 result of insufficient time for woody biomass to develop. Land cover alone cannot confidently serve as a proxy
192 for ecosystem recovery.

193 **S1.3 The effect of varying abandonment definitions**

194 A relatively short-term definition of abandonment might result in an overestimation of recultivation, because
195 short-term abandonment may be better understood as cyclical fallow periods, not true abandonment.²
196 Because typical fallow period length may vary around the world, we tested multiple abandonment thresholds
197 in order to test the sensitivity of our results to our choice of a five-year abandonment definition, following the
198 FAO.³ As our abandonment threshold increased in length, the mean abandonment duration across our sites
199 increased accordingly, ranging between 7 years (no threshold) and 19 years (10-year threshold). As expected,
200 using a longer abandonment definition reduced the amount of cropland abandonment we detected, which is
201 also shown in the area in the different colored age classes in Figure S3.

202 The proportion of abandoned croplands that were recultivated by the end of the time series also responded to
203 our abandonment threshold, with less recultivation for longer abandonment thresholds (Figure S11). However,
204 even at the longest abandonment definition (10 years), we still saw that between 10% and 30% of abandoned
205 croplands were recultivated by the end of the time series. We find that the mean area of abandoned croplands
206 that get recultivated by the end of the time series declines from 37.77% with a 5 year threshold to 30.93%
207 with a 7 year threshold, and 22.83% with a 10 year threshold. This indicates that the abandonment and
208 recultivation we observe is not merely a function of our five-year abandonment definition.

209 **S1.4 Comparing annual and two-year estimates of abandonment**

210 Some studies estimate cropland abandonment by simply looking for areas where land cover is classified as
211 “cultivated” in one year, but not in a later year (e.g., 1992 and 2015 in ref.).⁴ In order to understand the
212 magnitude of the differences that could result from using this two-year approach, we estimated cropland
213 abandonment by simply identifying areas that were classified as “cropland” in 1987 and classified as either
214 “woody vegetation” or “herbaceous vegetation” in 2017 (i.e., excluding “non-vegetation”).

215 Table S2 shows the area of abandoned croplands as identified using a five-year abandonment definition and the
216 full annual time series (Column 2), and the area of abandoned croplands identified using only the difference
217 between 2017 and 1987 (Column 3). These two methods produced abandonment area estimates that ranged
218 between 39.75% lower (Goiás, Brazil) and 83.29% higher (Mato Grosso, Brazil) than the abandoned area
219 identified using the full time series.

220 Not only do these methods produce different area estimates, but they also differ in the location of the
221 abandonment they identify, with spatial agreement of only 28.08% (Mato Grosso, Brazil) to 66.3% (Bosnia &
222 Herzegovina) (see Table S2). We measure spatial agreement using the Jaccard similarity index [Legendre2012],
223 a measure of overlap between two sets, defined as the proportion of shared elements, or the intersection
224 divided by the union (Equation (S1)):⁵

$$J(a, b) = \frac{a \cap b}{a \cup b} \quad (\text{S1})$$

225 **S1.5 Maps of abandonment duration as of 2017 and maximum duration during 226 time series**

227 As described in the main text, because a pixel may be abandoned and recultivated multiple times throughout
228 the time series, we calculated the mean abandonment duration in two ways: 1) across all periods of
229 abandonment (as shown in Figure 2), and 2) across only the longest period of abandonment experienced by

²³⁰ each pixel. Maps of the maximum abandonment duration at each pixel at each site is shown in Figure S7
²³¹ (serving as a companion to Figure 1). The distribution of maximum duration values, and the corresponding
²³² mean maximum duration value at each site, is shown in Figure S6 (serving as a companion to Figure 2).
²³³ Expanded site-specific results are shown in Figures S27-S37.

²³⁴ **S2 Extended Methods**

²³⁵ As noted in our main text, we build on annual land cover maps for 1987-2017 developed by Yin et al.⁶
²³⁶ The following section outlines our data processing and analytical methods in more specific detail than was
²³⁷ possible in the main text. We processed and analyzed our abandonment map data in RStudio version
²³⁸ 1.4.1717,⁷ using R version 4.1.0 (2021-05-18), relying heavily on the `{raster}`,⁸ `{terra}`,⁹ `{data.table}`,¹⁰
²³⁹ and `{tidyverse}`¹¹ packages.

²⁴⁰ **S2.1 Classifying abandonment**

²⁴¹ Pixels that remained in cropland or non-cropland classes throughout the entire time series were excluded,
²⁴² as were periods of non-cropland that began in the first year of the time series, even if that pixel was later
²⁴³ classified as cropland and subsequently abandoned. In effect, we only counted periods of abandonment that
²⁴⁴ we could verify had followed agricultural activity during our time series.

²⁴⁵ As noted, pixels that transitioned from cropland to the non-vegetation land cover class were not considered
²⁴⁶ “abandoned,” and therefore we excluded all non-vegetation pixels from our entire analysis. These pixels
²⁴⁷ accounted for <10% of total site area at all sites except Shaanxi (12.7%) and Iraq (52.8%), and remained
²⁴⁸ stable or declined over time at all eleven sites (see Figure S4).

²⁴⁹ All area calculations were performed using the `{terra}` package’s `cellSize()` function, which calculates the
²⁵⁰ spherical area of each cell as defined by its four corners.⁹

²⁵¹ **S2.2 Temporal filters**

²⁵² In order to address potential classification errors in a single year, we implemented a series of temporal filters
²⁵³ designed to smooth trajectories by looking for short-term land-cover changes that are temporally unlikely.
²⁵⁴ We applied five-year and eight-year moving-window filters that searched for short periods of land cover
²⁵⁵ classifications that do not match those immediately before and after, and subsequently updated them to match
²⁵⁶ the surrounding classifications. Specifically, the five-year filter searched for one year periods that did not
²⁵⁷ match the two years immediately before and after (i.e., patterns of 11011, where 1 represents non-cropland
²⁵⁸ and 0 represents cropland), and our eight-year filter searched for two year periods that did not match the
²⁵⁹ three years before and after (i.e., 11100111). The central classifications were then updated to match the
²⁶⁰ classes on either end.

²⁶¹ **S2.3 Modeling abandonment decay**

²⁶² Our mean abandonment duration metric tells us about the general persistence of abandoned croplands
²⁶³ throughout the time series. However, this value is limited by the time series length, and does not account for
²⁶⁴ when the majority of the abandonment took place at a site, nor whether a period of abandonment ends as a
²⁶⁵ results of recultivation or the end of the time series. As a result, the mean abandonment duration does not
²⁶⁶ tell us how long to expect a piece of land to remain abandoned, nor how abandonment length varies through
²⁶⁷ time. To address this constraint, we track the trajectory of each pixel through time following its initial
²⁶⁸ abandonment, grouping pixels abandoned in a given year into “cohorts.” Decay rates provide information
²⁶⁹ about how long it takes for land to be recultivated, complementing the mean abandonment length and
²⁷⁰ providing a more nuanced story about how long to expect abandonment to last.

271 For example, a site may have a relatively short mean length of abandonment (e.g., Shaanxi/Shanxi [China],
 272 with a mean abandonment length of 13 years; see Figure 1), but also have a gradual decay rate, indicating that
 273 land should stay abandoned for a relatively longer amount of time. This may result from more abandonment
 274 occurring towards the end of the time series; this land simply does not have as long to age and shows up as
 275 younger in our data, regardless of how long it may last. Looking at abandonment decay rates for each cohort
 276 individually allows us to produce a decay rate for each site in general in a way that accounts for when during
 277 the time series a piece of land was abandoned (i.e., giving us a sense of how long to expect a given piece of
 278 land to remain abandoned, even into the future).

279 S2.3.1 Model selection and diagnostics

280 We fit linear models using the `lm()` function in R's core statistics package `{stats}`, predicting the proportion
 281 of abandoned cropland in each cohort remaining abandoned as a function of time since initial abandonment
 282 at each site. The proportion of abandoned cropland remaining abandoned is measured relative to the area
 283 abandoned 5 years following the year of initial abandonment, as dictated by our five year abandonment
 284 definition.

285 We tested a range of model specifications, including linear and log transformations of both *proportion* and
 286 *time*. Due to a linear relationship between model residuals and time when including only one term for *time*,
 287 we also tested models containing multiple *time* predictor terms, including both log and linear terms.

288 We chose a model with the following specifications shown in Equation 1 and reproduced here in Equation
 289 (S2). For cohorts of abandonment initially abandoned in years $y = 1988, \dots, 2013$, we estimate the proportion
 290 p of each cohort y remaining abandoned as a function of time t (i.e., based on the number of years after
 291 initial abandonment).

$$p_y = 1 + \beta_{1,y} \log(t + 1) + \beta_{2,y} t \quad (\text{S2})$$

292 Where $\beta_{1,y}$ represents the regression coefficient on the log term of time t for cohort y , and $\beta_{2,y}$ represents the
 293 regression coefficient on the linear term of time t for cohort y . We allow for *cohort* level fixed effects, fitting
 294 unique coefficients for each cohort at each site. We ran individual models for each site, using a `stats::lm()`
 295 call of `lm(formula = I(proportion - 1) ~ 0 + log(time + 1):cohort + I(time):cohort)` on data
 296 for only that site. Taken together, these 11 models correspond to a `stats::lm()` call of `lm(formula =`
 297 `I(proportion - 1) ~ 0 + log(time + 1):cohort:site + I(time):cohort:site)`.

298 Model selection was performed based on Akaike Information Criterion (AIC) values (Figure S13), selecting
 299 the model with the lowest (i.e., more negative) AIC value. We confirmed that linear model assumptions were
 300 not violated through visual inspection of both residuals vs. fitted plots (Figure S14) and Q-Q plots (Figure
 301 S15).

302 S2.3.2 Recultivation (“decay”) model results

303 The observed data, fitted values from these linear models, and mean decay rates for each site, are shown in
 304 Figure S12.

305 In order to calculate the mean decay trajectory at each site (as shown in Figure 3), we took the mean of the
 306 log coefficients ($\beta_{1,\bar{y}}$) and the linear coefficients ($\beta_{2,\bar{y}}$) respectively across all cohorts y at each site. These
 307 mean values are shown in Figure S16. We then used these mean coefficient values ($\beta_{1,\bar{y}}$ and $\beta_{2,\bar{y}}$) to define
 308 a new function describing the mean recultivation (or decay) trajectory at each site, using the same for as
 309 Equation (S2).

310 An alternative representation of the mean recultivation rate is shown in Figure S17.

311 **S2.4 Change in recultivation rates over time**

312 We examined the rate of change of recultivation rates by calculating the half-life, $t_{half,s}$, defined as the time
313 required for half (50%) of a given cohort of abandoned cropland to be recultivated, and parameterizing a
314 simple linear model on these half-life values as a function of time, using the `stats::lm()` function in R's core
315 statistics package `{stats}`. We estimate the half-life, $t_{half,s}$, as a function of the year of initial abandonment
316 ($yearabn_s$), at each site s , as shown in Equation (S3).

$$t_{half,s} = \beta_{0,s} + \beta_{1,s} yearabn_s \quad (S3)$$

317 Where $\beta_{1,s}$ represents the regression slope on the year abandoned (cohort) for site s ($yearabn_s$), and $\beta_{0,s}$ repre-
318 sents the intercept. This corresponds to a `stats::lm()` call of `lm(formula = t_half ~ year_abandoned)`,
319 run for each site individually. Results are shown in Figure S18.
320 We confirmed that model assumptions were met through visual inspection of residuals vs. fitted plots (Figure
321 S19) and Q-Q plots (Figure S20).

322 **S2.5 Projecting abandonment duration into the future**

323 The results of the projection highlighted in the main text (referred to here as “Extrapolation 1”) are shown in
324 Figure S22 and Figure S23. As noted in the main text, we make two simple assumptions in our projection of
325 abandonment and recultivation into the future: specifically, that 1) recultivation rates remain the same (based
326 on mean recultivation trends at each site, shown in Figure 3, and that 2) a constant amount of cropland is
327 newly abandoned each year, based on the mean annual gain in abandonment shown in Figure S21b (note:
328 the annual gain in abandonment in Figure S21a corresponds to the dark green bars in Figure S5).
329 Given that abandonment may not continue indefinitely, we also explore an alternative to our second assumption
330 about the amount of additional abandonment each year. In this alternative assumption (“Extrapolation 2”),
331 the area abandoned each year is the same as “Extrapolation 1” from 1987-2017, based on the mean annual
332 gain in abandonment (Figure S21b), but linearly declines between 2017-2050, reaching 0 ha at each site in
333 2050 (see Figures S24 and S25).
334 While mean age of abandoned land increased through time after 2017 (and most dramatically after 2050),
335 it remained below 37 years at all sites by 2050. Increases in mean abandonment duration were offset by
336 recultivation, and total area abandoned declined quickly after 2020 at most sites. The mean abandonment
337 duration increases as annual abandonment declines, as the total pool of abandoned land grows older and is
338 gradually recultivated.

339 **References**

- 340 1. Prach, K. & Walker, L. R. Differences between primary and secondary plant succession among biomes
341 of the world. *Journal of Ecology* 510–516 (2018) doi:[10.1111/1365-2745.13078](https://doi.org/10.1111/1365-2745.13078).
- 342 2. Munroe, D. K., Berkel, D. B. van, Verburg, P. H. & Olson, J. L. Alternative trajectories of land
343 abandonment: Causes, consequences and research challenges. *Current Opinion in Environmental
Sustainability* 5, 471–476 (2013).
- 344 3. Food and Agriculture Organization of the United Nations (FAO). FAOSTAT Statistical Database:
345 Methods & Standards. (2016).
- 346 4. Næss, J. S., Cavalett, O. & Cherubini, F. The land–energy–water nexus of global bioenergy potentials
347 from abandoned cropland. *Nature Sustainability* (2021) doi:[10.1038/s41893-020-00680-5](https://doi.org/10.1038/s41893-020-00680-5).
- 348 5. Legendre, P. & Legendre, L. *Numerical ecology*. 990 (Boston: Elsevier, 2012).
- 349
- 350 6. Yin, H. *et al.* Monitoring cropland abandonment with Landsat time series. *Remote Sensing of
351 Environment* 246, 111873 (2020).
- 352 7. RStudio Team. RStudio: Integrated Development Environment for R. (2020).
- 353
- 354 8. Hijmans, R. J. *Raster: Geographic data analysis and modeling*. (2021).
- 355
- 356 9. Hijmans, R. J. *Terra: Spatial data analysis*. (2021).
- 357
- 358 10. Dowle, M. & Srinivasan, A. *Data.table: Extension of ‘data.frame’*. (2021).
- 359
- 360 11. Wickham, H. *Tidyverse: Easily install and load the tidyverse*. (2021).
- 361
- 362 12. Olson, D. M. *et al.* Terrestrial Ecoregions of the World: A New Map of Life on Earth. *BioScience* 51,
363 933–938 (2001).
- 364 13. Olson, D. M. & Dinerstein, E. The Global 200: Priority ecoregions for global conservation. *Annals of
365 the Missouri Botanical Garden* 89, 199–224 (2002).
- 366 14. Fox, J., Weisberg, S. & Price, B. *Car: Companion to applied regression*. (2021).
- 367

³⁶⁸ S3 Supplementary Tables

Table S1: Summary statistics describing the duration of abandonment (in years) at our eleven sites between 1987 and 2017, using a five year abandonment definition, and incorporating all periods of abandonment (allowing for multiple per pixel).

	Site	Mean	Median	Standard Deviation
Vitebsk, Belarus / Smolensk, Russia		13.87	12	7.60
Bosnia & Herzegovina		17.70	18	8.36
Chongqing, China		12.92	11	7.32
Goiás, Brazil		13.61	12	7.42
Iraq		15.72	13	8.78
Mato Grosso, Brazil		15.30	11	9.21
Nebraska/Wyoming, USA		15.32	14	8.04
Orenburg, Russia / Uralsk, Kazakhstan		12.86	11	6.95
Shaanxi/Shanxi, China		13.00	11	7.15
Volgograd, Russia		13.33	12	7.01
Wisconsin, USA		15.00	14	7.78

Table S2: Cropland abandonment (in Mha) as of 2017 as identified using a) our annual time series and a five-year abandonment definition and b) a two year method taking the difference between land cover in 1987 and 2017.

	Site	Area (annual, as of 2017)	Area (two year: 2017-1987)	Percent Difference	Jaccard Similarity
Goiás, Brazil		530,252	319,499	-39.75%	0.29
Vitebsk, Belarus / Smolensk, Russia		917,934	655,689	-28.57%	0.51
Chongqing, China		382,125	273,839	-28.34%	0.43
Nebraska/Wyoming, USA		351,006	274,133	-21.9%	0.50
Bosnia & Herzegovina		690,376	569,091	-17.57%	0.66
Wisconsin, USA		411,833	358,420	-12.97%	0.48
Iraq		368,103	348,152	-5.42%	0.54
Volgograd, Russia		828,276	857,989	3.59%	0.47
Orenburg, Russia / Uralsk, Kazakhstan		930,424	975,131	4.8%	0.52
Shaanxi/Shanxi, China		314,375	355,581	13.11%	0.49
Mato Grosso, Brazil		9,006	16,507	83.29%	0.28

³⁶⁹ S4 Supplementary Figures

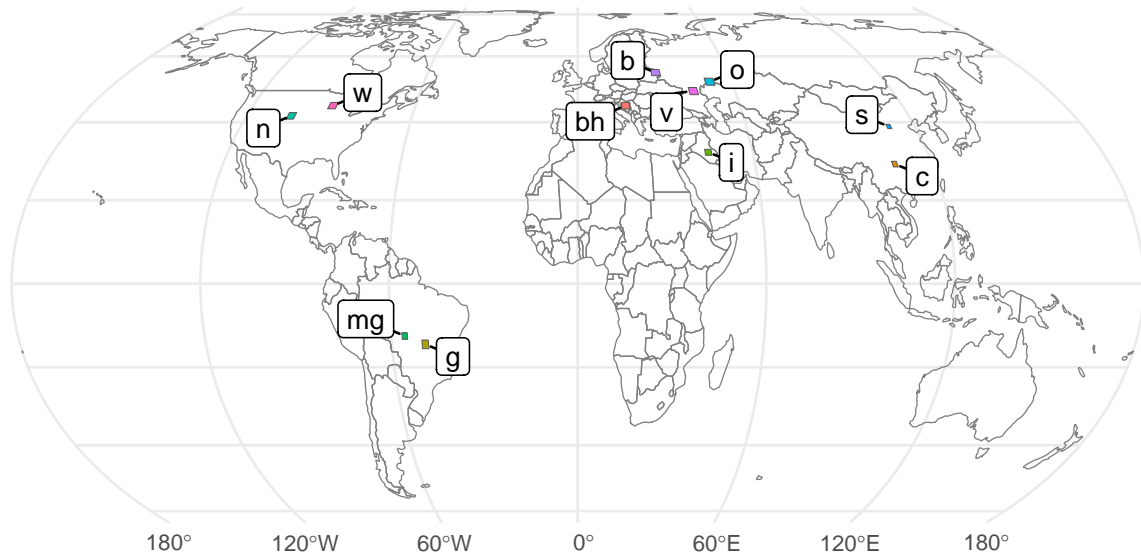


Figure S1: The locations of our 11 sites, from Yin et al.⁶ Sites are labeled as follows: (b) Vitebsk, Belarus / Smolensk, Russia; (bh) Bosnia & Herzegovina; (c) Chongqing, China; (g) Goiás, Brazil; (i) Iraq; (mg) Mato Grosso, Brazil; (n) Nebraska/Wyoming, USA; (o) Orenburg, Russia / Uralsk, Kazakhstan; (s) Shaanxi/Shanxi, China; (v) Volgograd, Russia; (w) Wisconsin, USA.

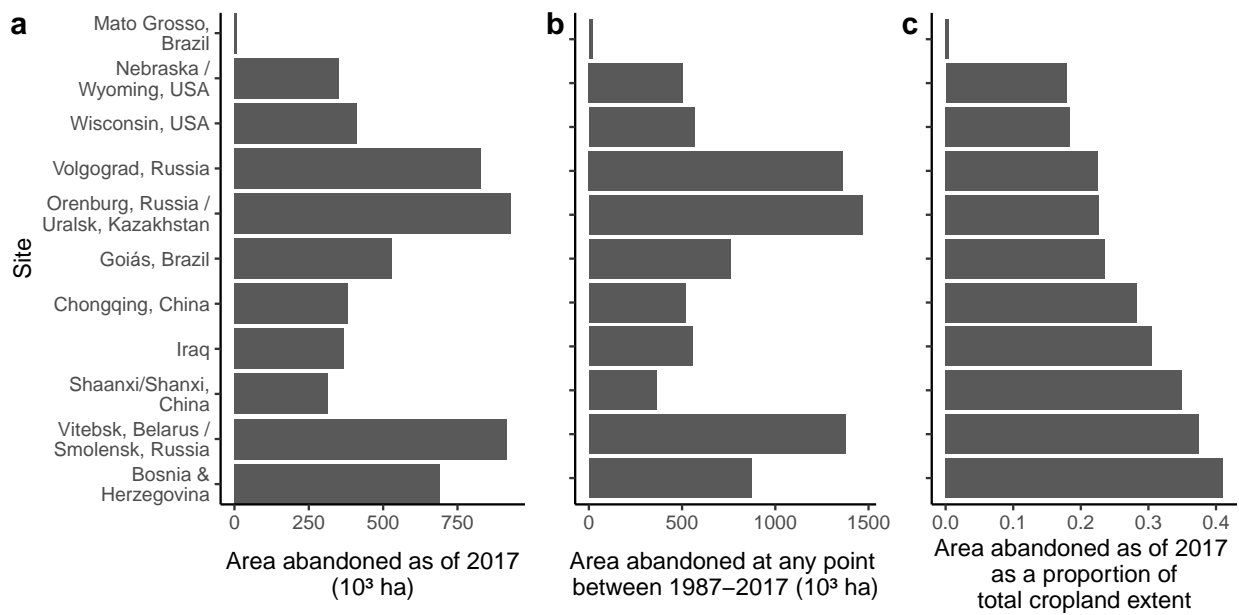


Figure S2: Area abandoned a) as of 2017, b) at any point between 1987–2017, c) as of 2017 as a proportion of the total cropland extent (i.e., the area of all lands that were cultivated at some point during the time series). Note that sites are shown in ascending order of area abandoned as of 2017 as a proportion of total cropland extent.

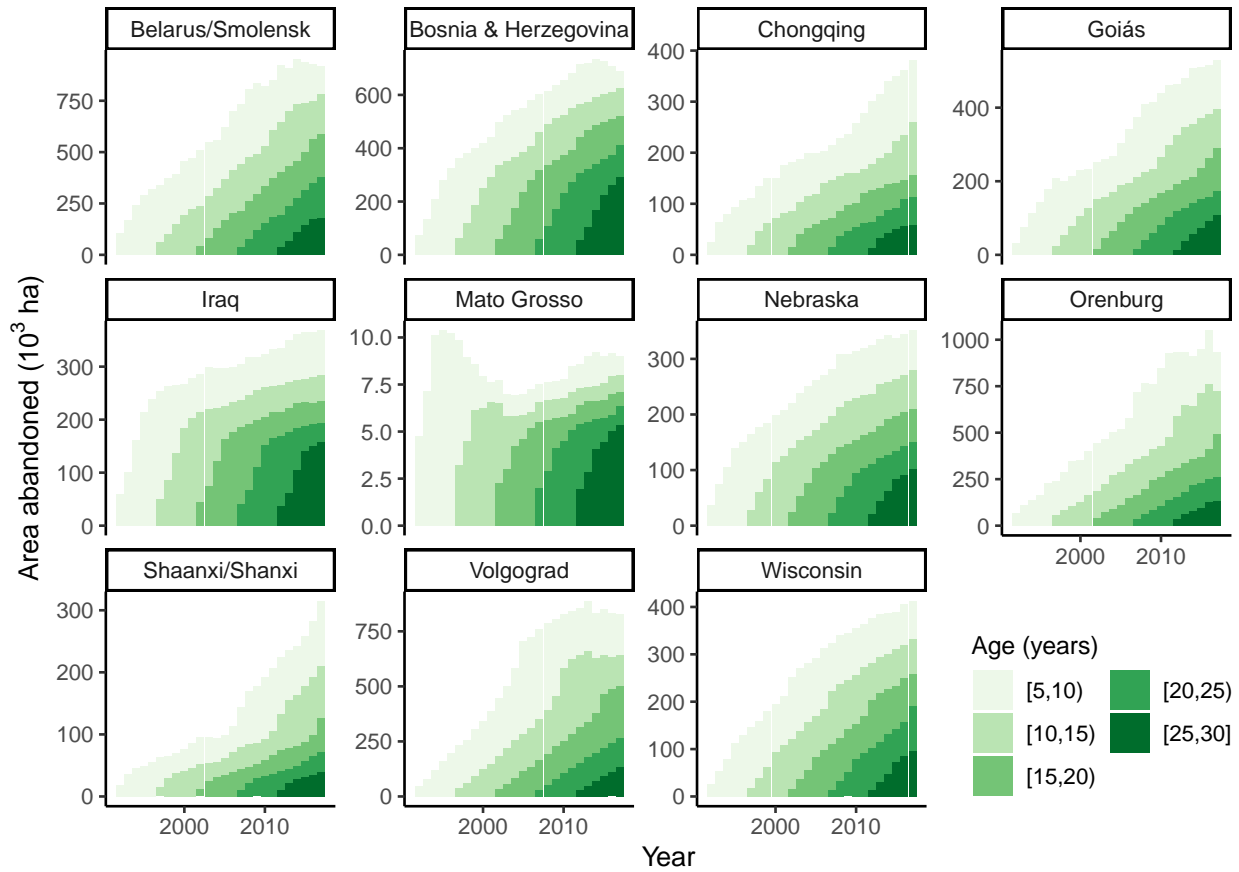


Figure S3: Cumulative area abandoned at each site through time, according to age class (in years).

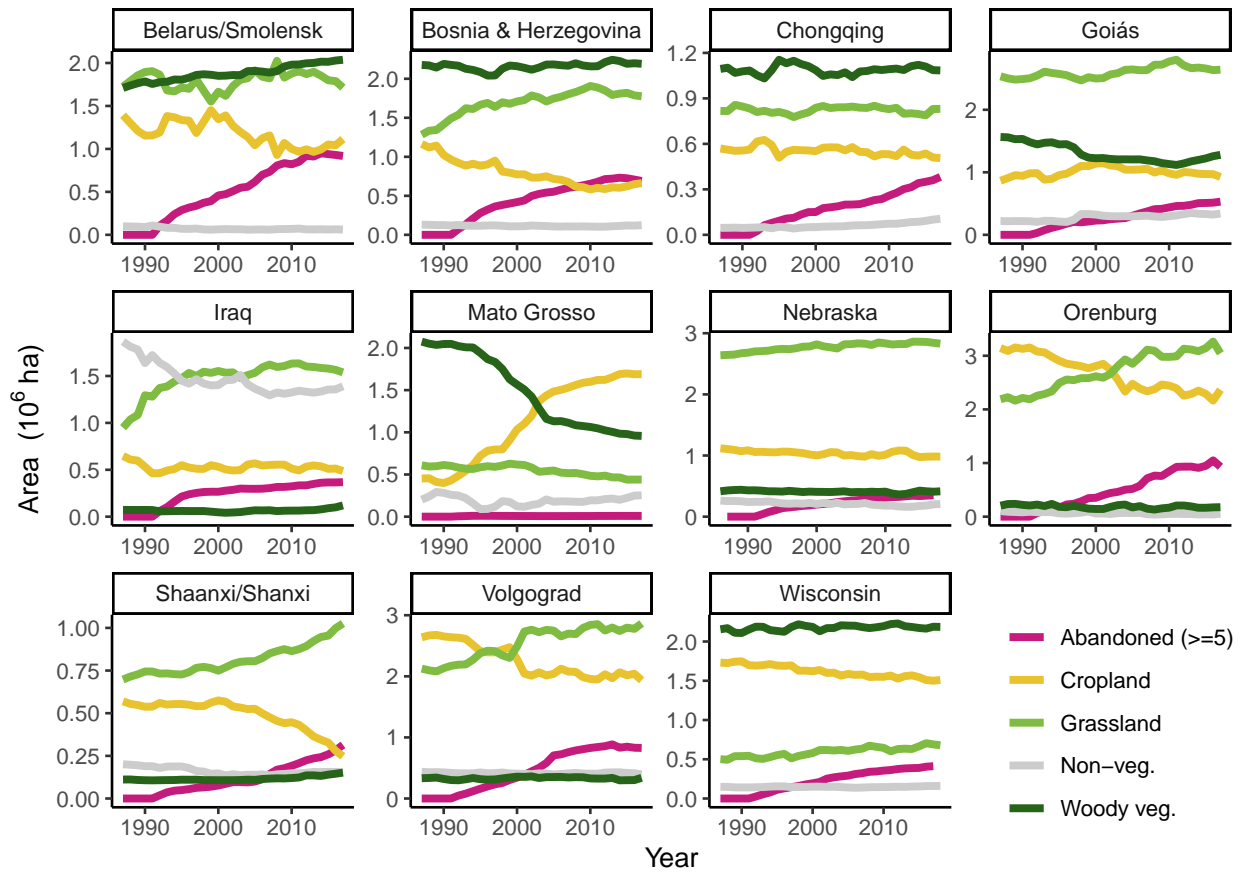


Figure S4: Area in each land cover class at each site through time. Land cover classes are cropland, grassland, woody vegetation, non-vegetation, and abandoned (for at least 5 years).

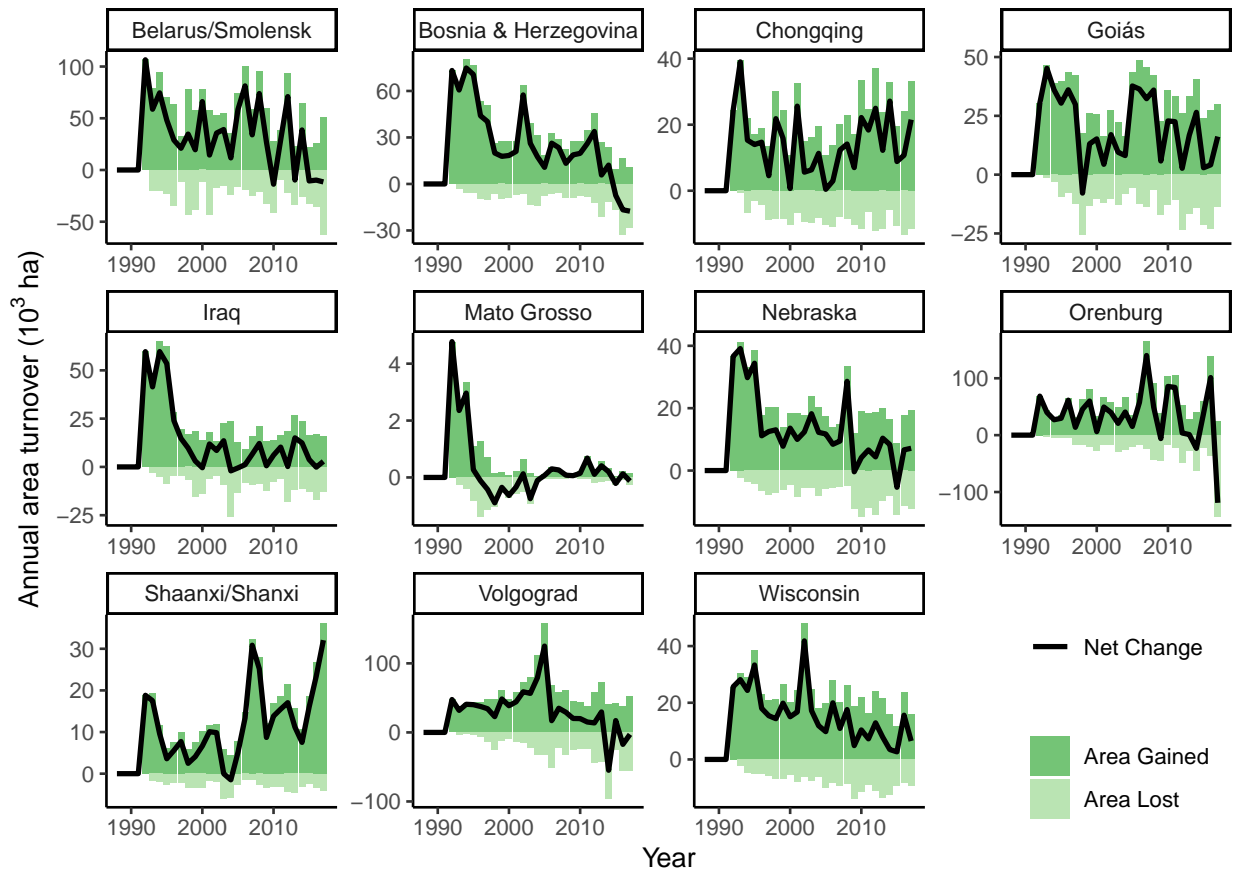


Figure S5: Annual turnover of abandoned croplands at each site, showing the annual gain (dark green) and annual loss (i.e., recultivation, light green) and net change (black line) of abandoned croplands.

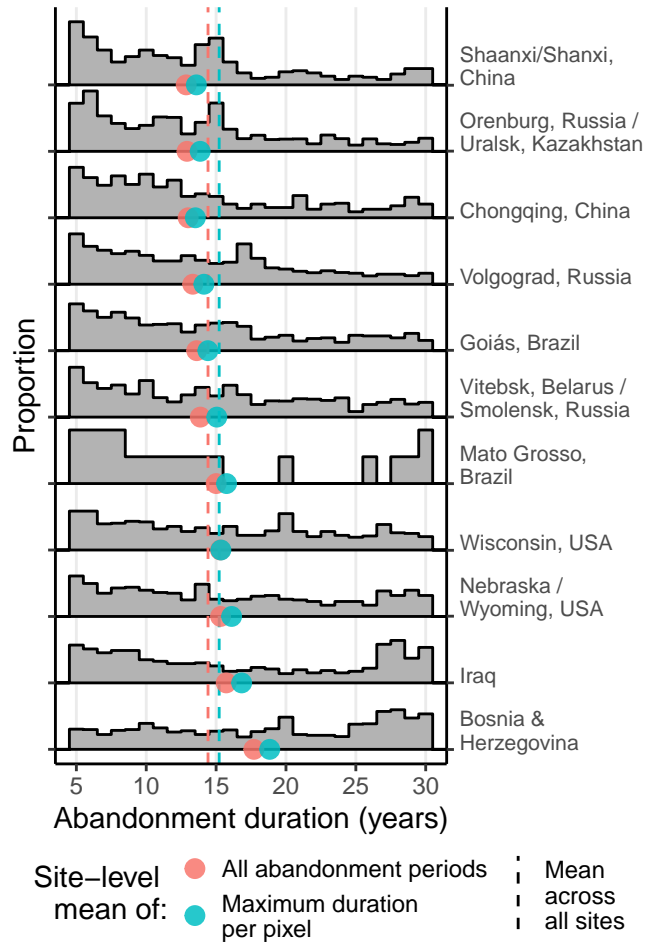


Figure S6: The distribution of the maximum abandonment duration (in years) for each pixel at each site from 1987 to 2017. The y-scale shows the proportion of pixels with maximum duration values of a given duration at each site. As previously noted, abandonment and recultivation can occur multiple times at a single pixel during our time series, and this figure serves as a companion to the distribution of all abandonment values shown in Figure 2. Site-level mean duration values are shown in the red and blue dots, corresponding to mean values calculated across all periods of abandonment (in red, including multiple periods per pixel) and mean values calculated across only the maximum duration of abandonment at each pixel (in blue). The vertical dashed lines represent the mean of these site-level mean duration values, for all abandonment periods (red) and only the maximum duration at each pixel (blue), respectively.

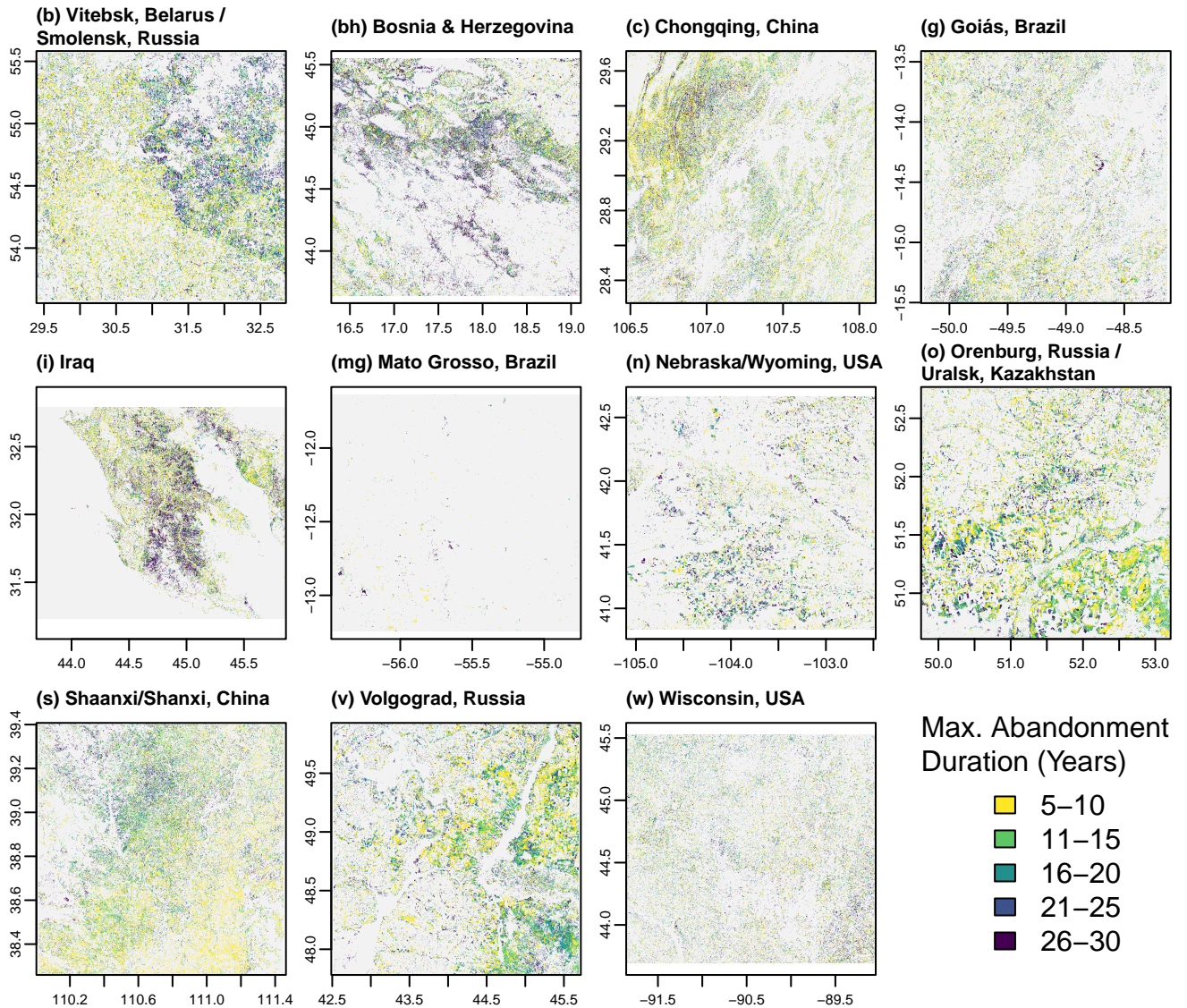


Figure S7: Maximum duration of cropland abandonment (in years) observed at each pixel between 1987 and 2017 in our eleven study sites. This serves as a companion to maps of the abandonment duration as of 2017 shown in Figure 1. Site locations are shown in Figure S1.

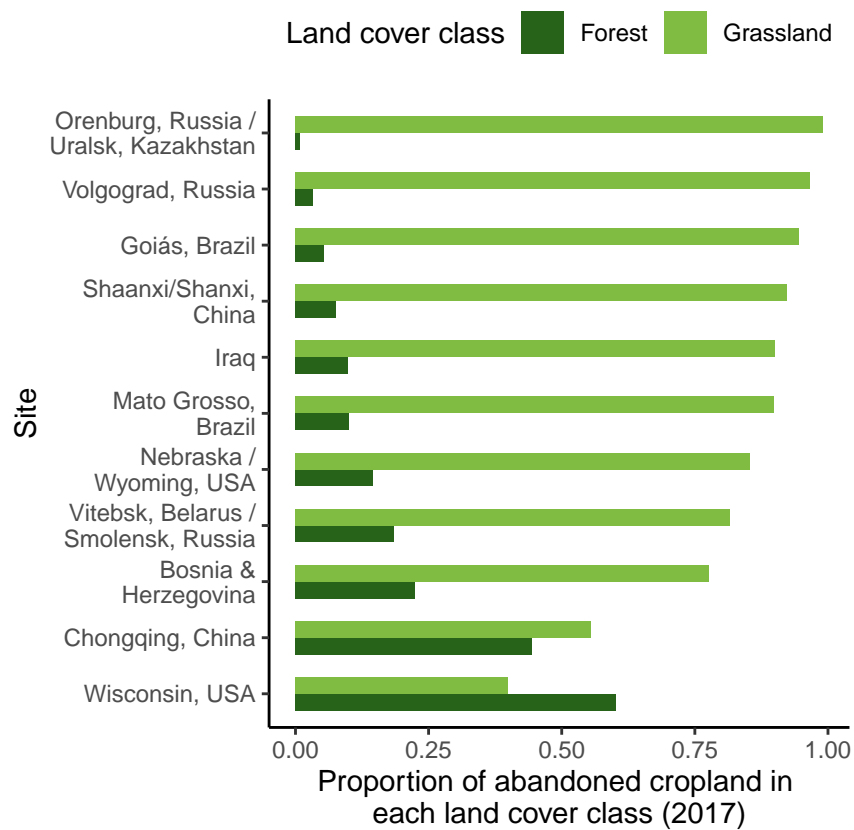


Figure S8: Proportion of abandoned cropland in each land cover class as of 2017.

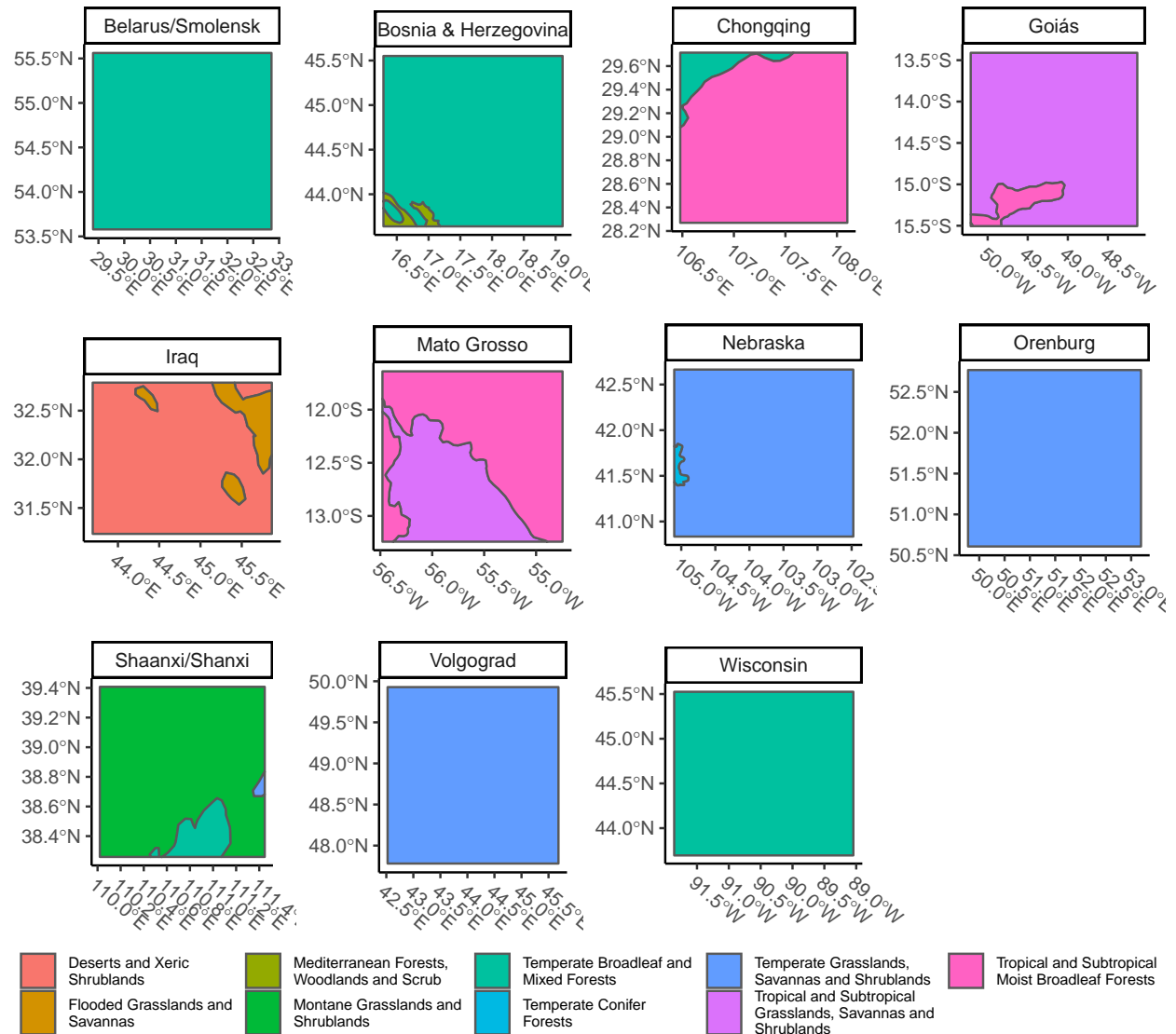


Figure S9: Site biomes, using biome classifications from The Nature Conservancy's Terrestrial Ecoregions of The World (TEOW) database, derived from Olson et al.¹² and Olson and Dinerstein.¹³

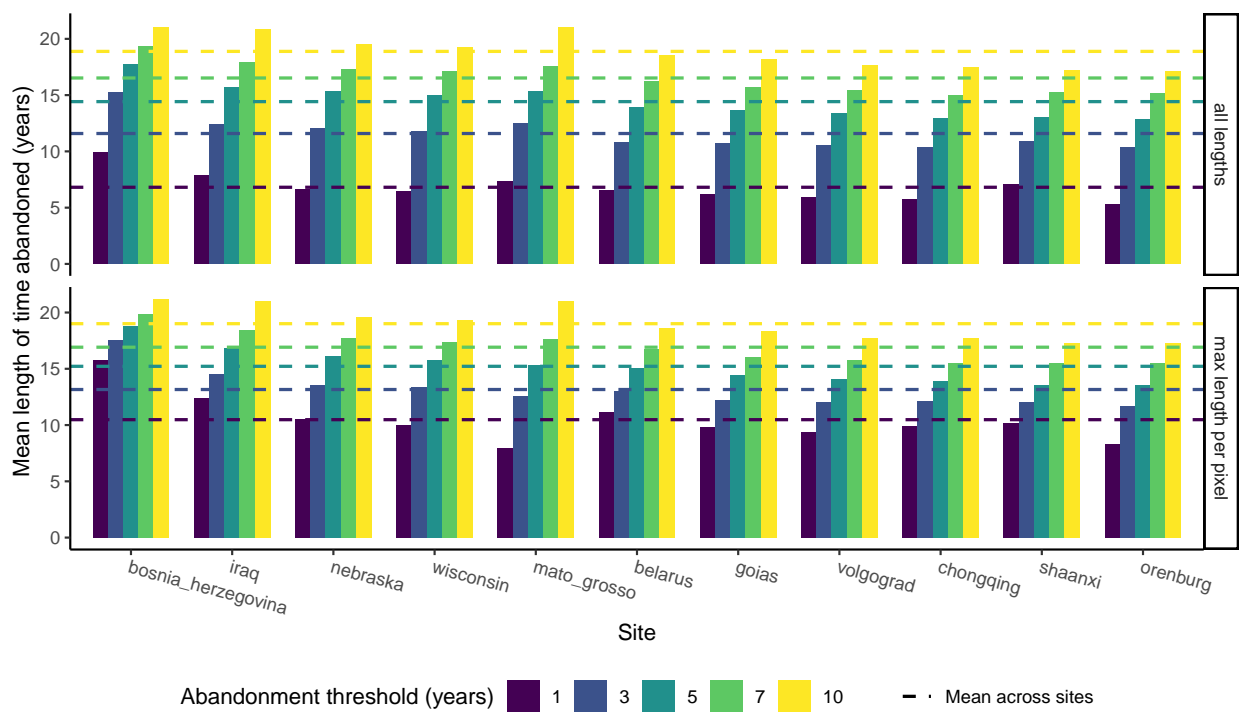


Figure S10: Mean abandonment lengths shown for various abandonment thresholds.

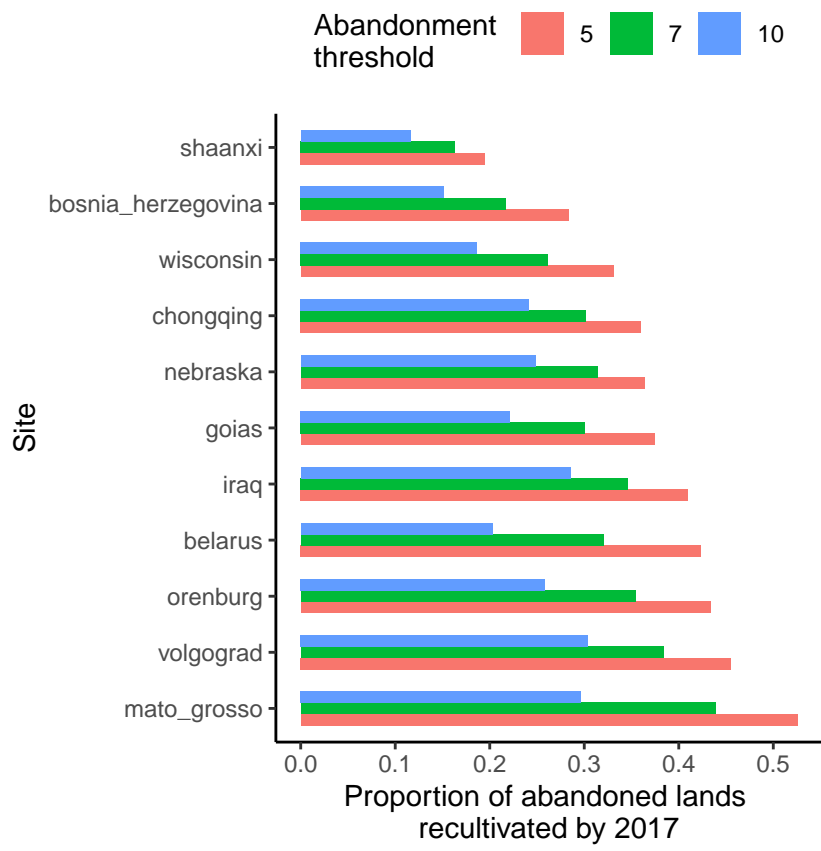


Figure S11: Recultivation rates shown for various abandonment thresholds.

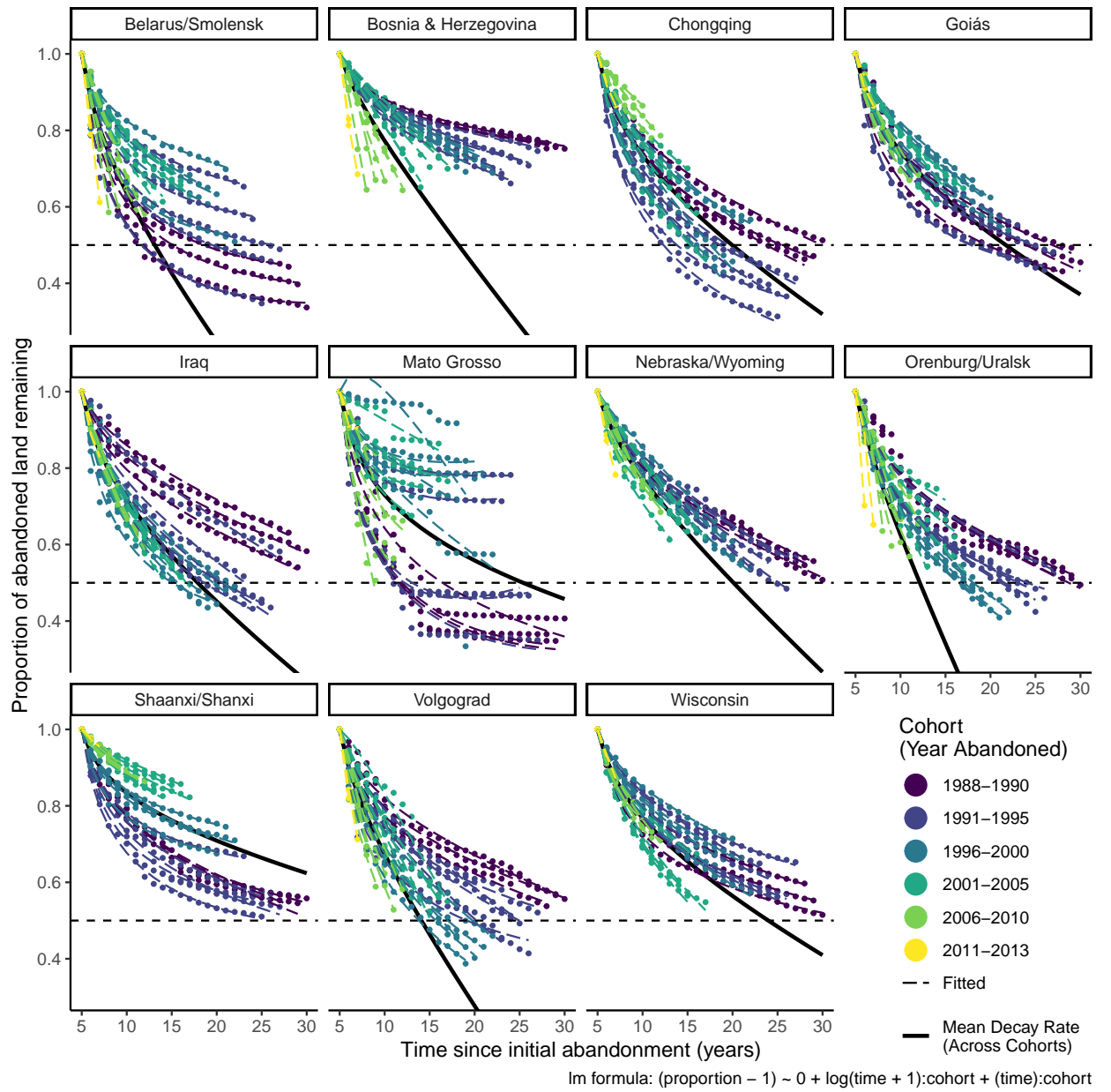


Figure S12: Decay model results for all sites, showing the proportion of each cohort of abandoned land (i.e., all pixels abandoned in a given year) remaining abandoned over time for each of our eleven sites. Points represent actual observations by cohort, dashed lines represent linear model predictions (fitted values) for each cohort as a function of time (including a linear and logarithmic term of time), and the solid black line represents the site-level mean trend across all cohorts (calculated by taking the mean of each time coefficient values across all cohorts, respectively, and using those two mean values to plot a mean trend). Colors of both points and dashed lines correspond to roughly five-year group of cohorts, ranging from dark purple (oldest cohorts) to green and yellow (most recent cohorts). The horizontal black dashed line shows a proportion of 0.5, indicating the point where half of a cohort has been recultivated. Model diagnostic plots are shown in Figures S14 and S15.

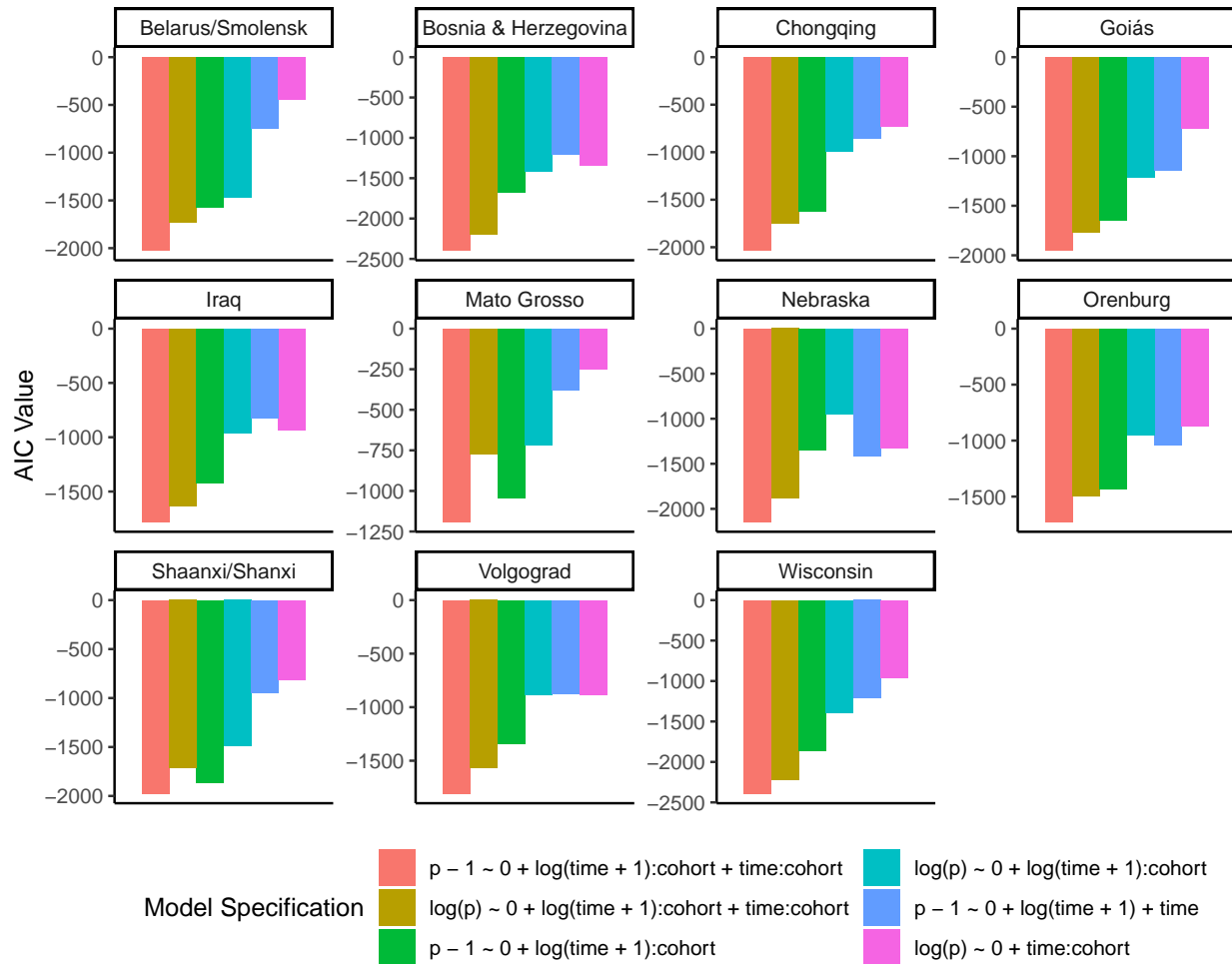


Figure S13: Akaike Information Criterion (AIC) values for various recultivation (“decay”) model specifications for each site. More negative AIC values indicate a better model fit.

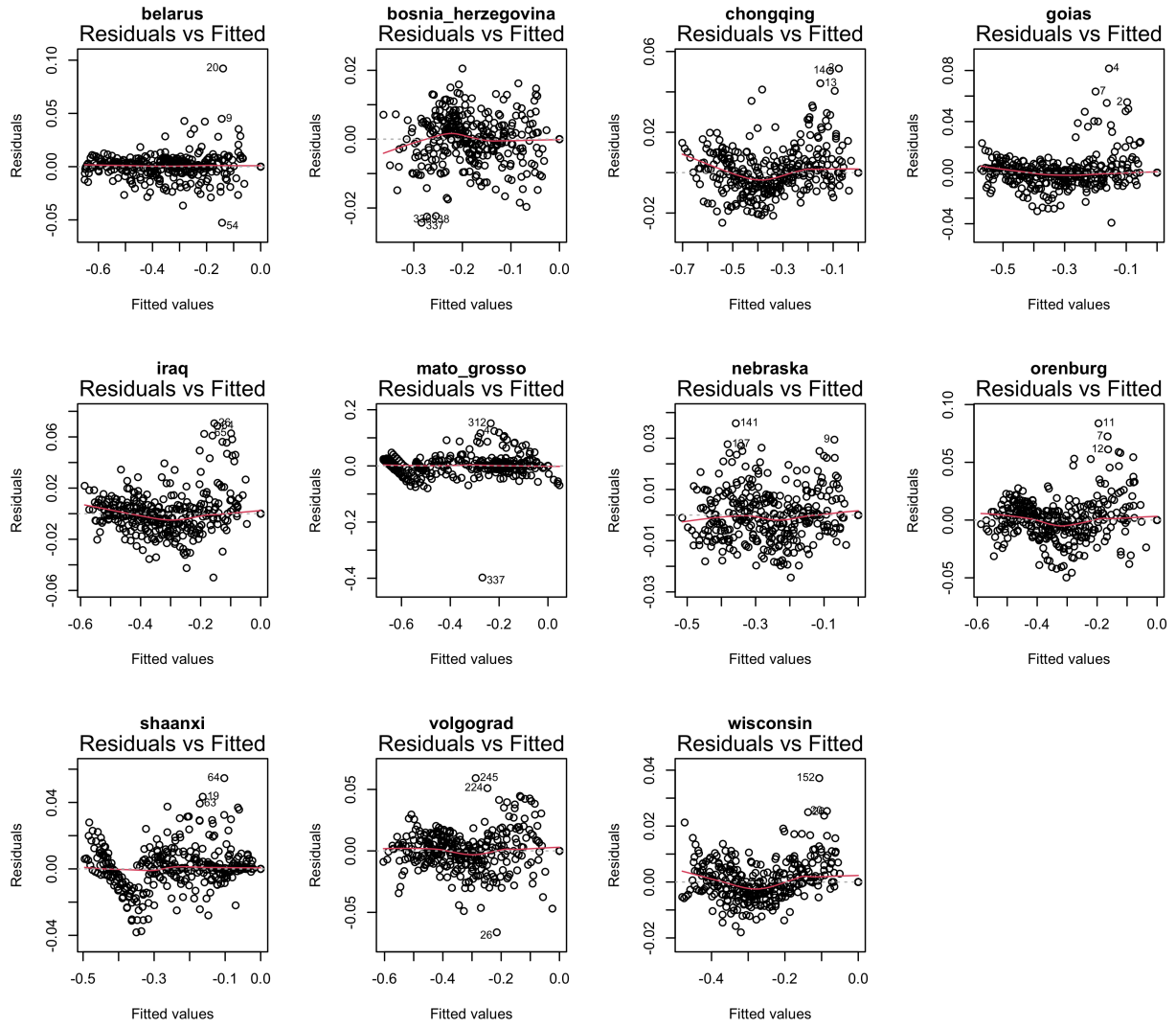


Figure S14: Residuals vs. fitted diagnostic plots for our linear models of the recultivation (“decay”) of abandonment at each site. These models take the form shown in Equation (S2), and are shown in Figure S12.

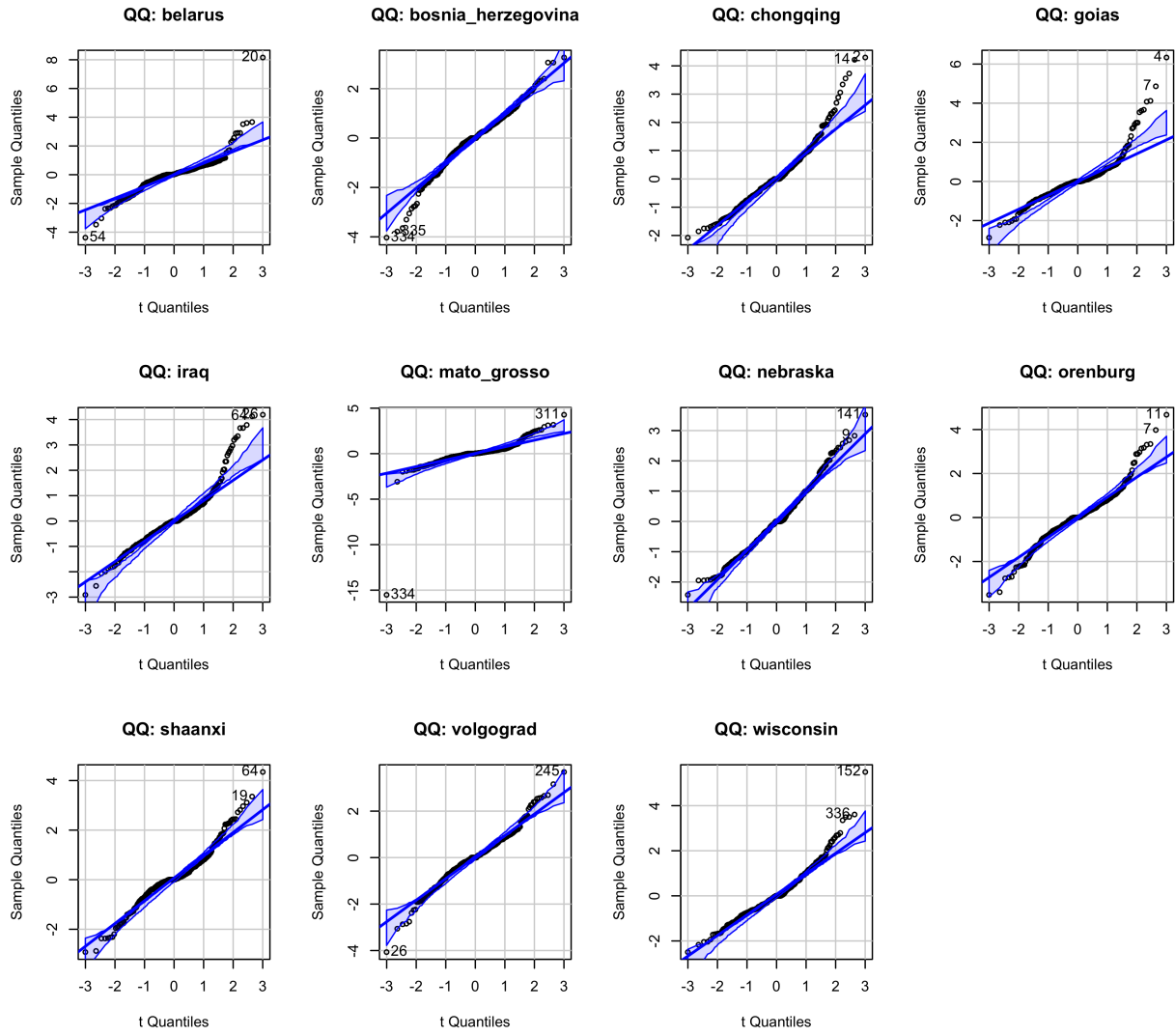


Figure S15: QQ plots calculated using the `{car}` package¹⁴ for our linear models of the recultivation (“decay”) of abandonment at each site. These models take the form shown in Equation (S2), and are shown in Figure S12.

Mean Decay Rates By Site

Im formula: $(\text{proportion} - 1) \sim 0 + \log(\text{time} + 1):\text{cohort} + (\text{time}):\text{cohort}$

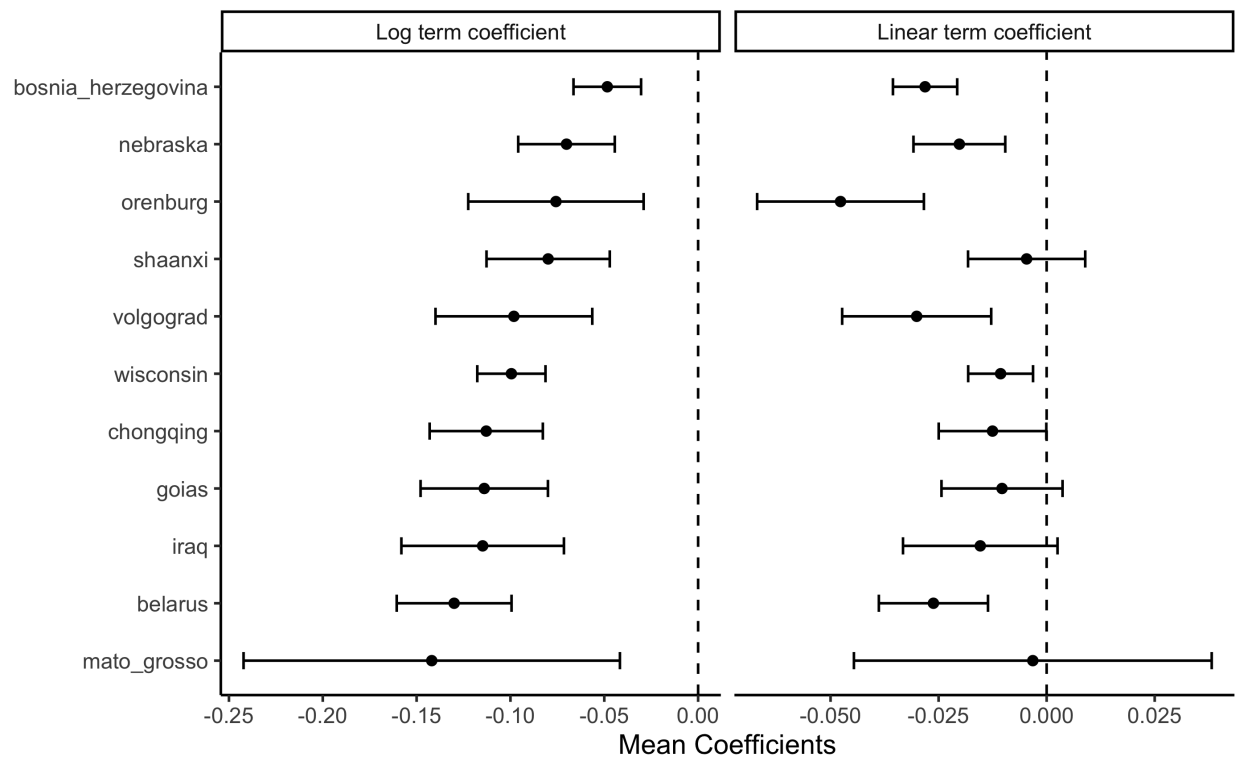


Figure S16: Mean decay model coefficients across cohorts at each site. The left panel shows the mean coefficient on the $\log(\text{time})$ terms and the right shows the site mean coefficient on the linear time terms. These mean coefficients are used to plot the mean decay trajectories shown in Figure 3.

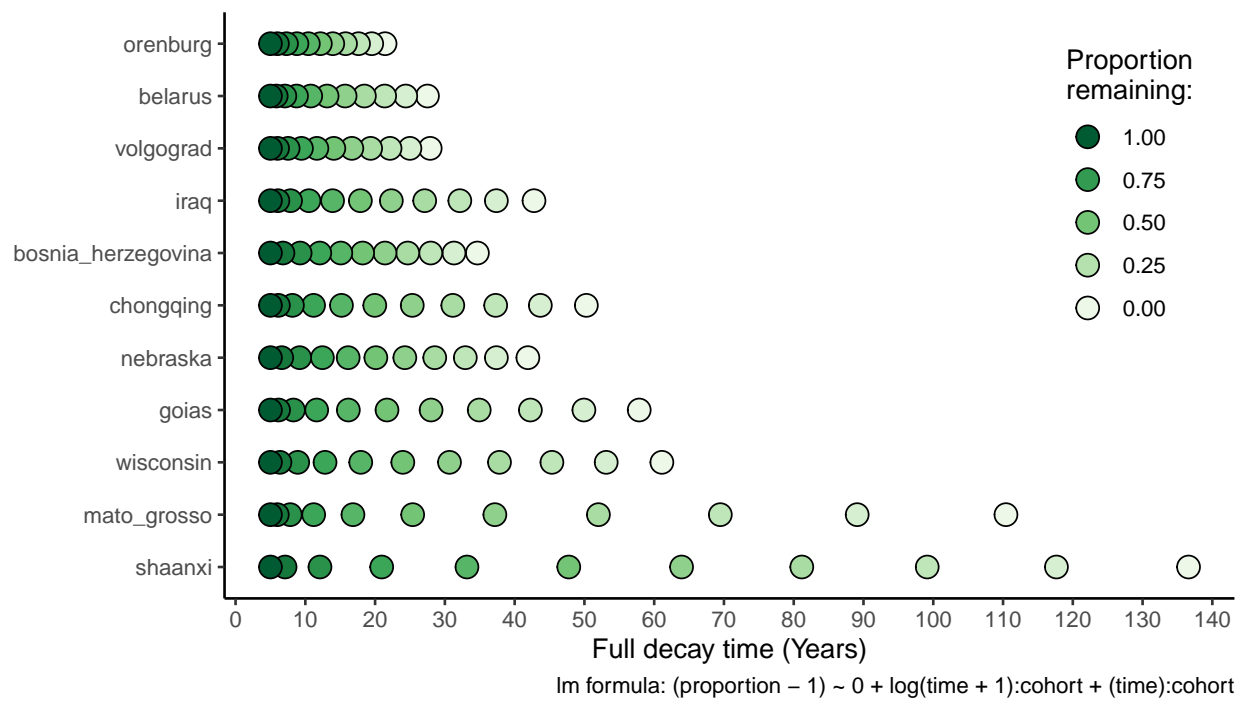


Figure S17: An alternative representation of the mean decay rate for each site (also shown in Figure 3). The color of each point corresponds to the proportion remaining after a given amount of time.

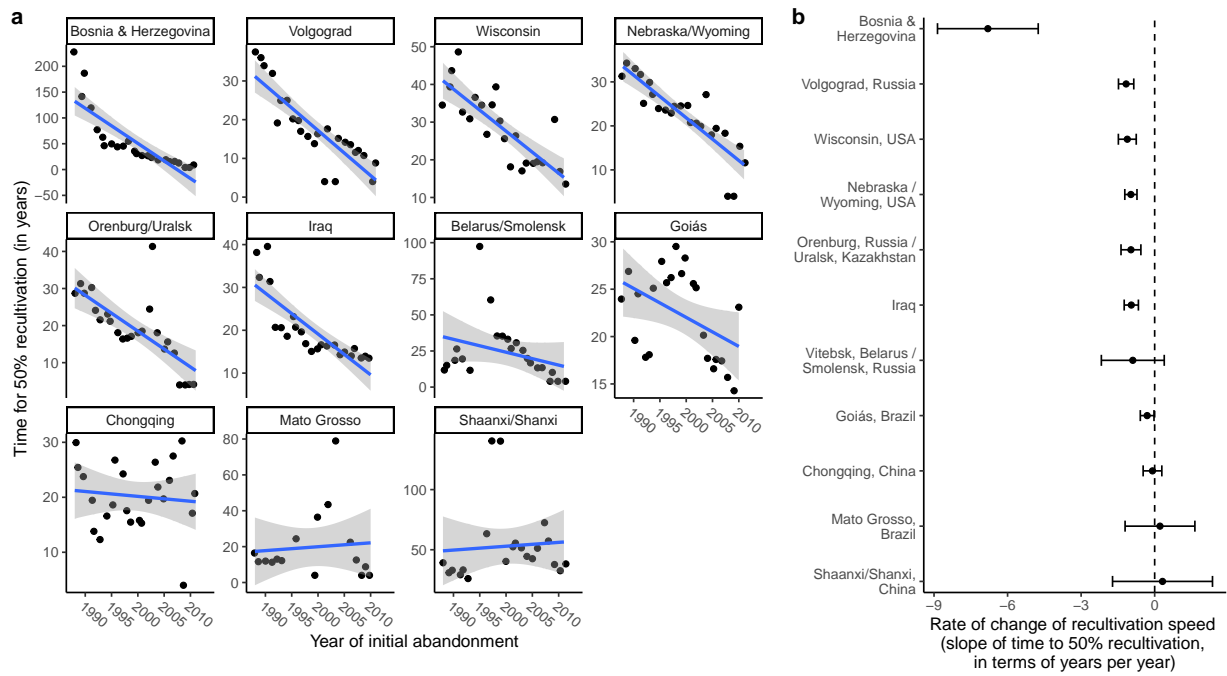


Figure S18: The rate of change of decay rates (measured as the half-life, or the time required for 50% of each cohort to be recultivated) at each site over the course of the time series. Individual site trends are shown in panel a. Solid lines show simple linear regressions, the slopes of which are shown in panel b. Gray bands around the linear trends in panel a and the error bars on slope estimates in panel b both represent 95% confidence intervals. These models are described by Eq. (S3). Model diagnostic plots are shown in Figures S19 and S20.

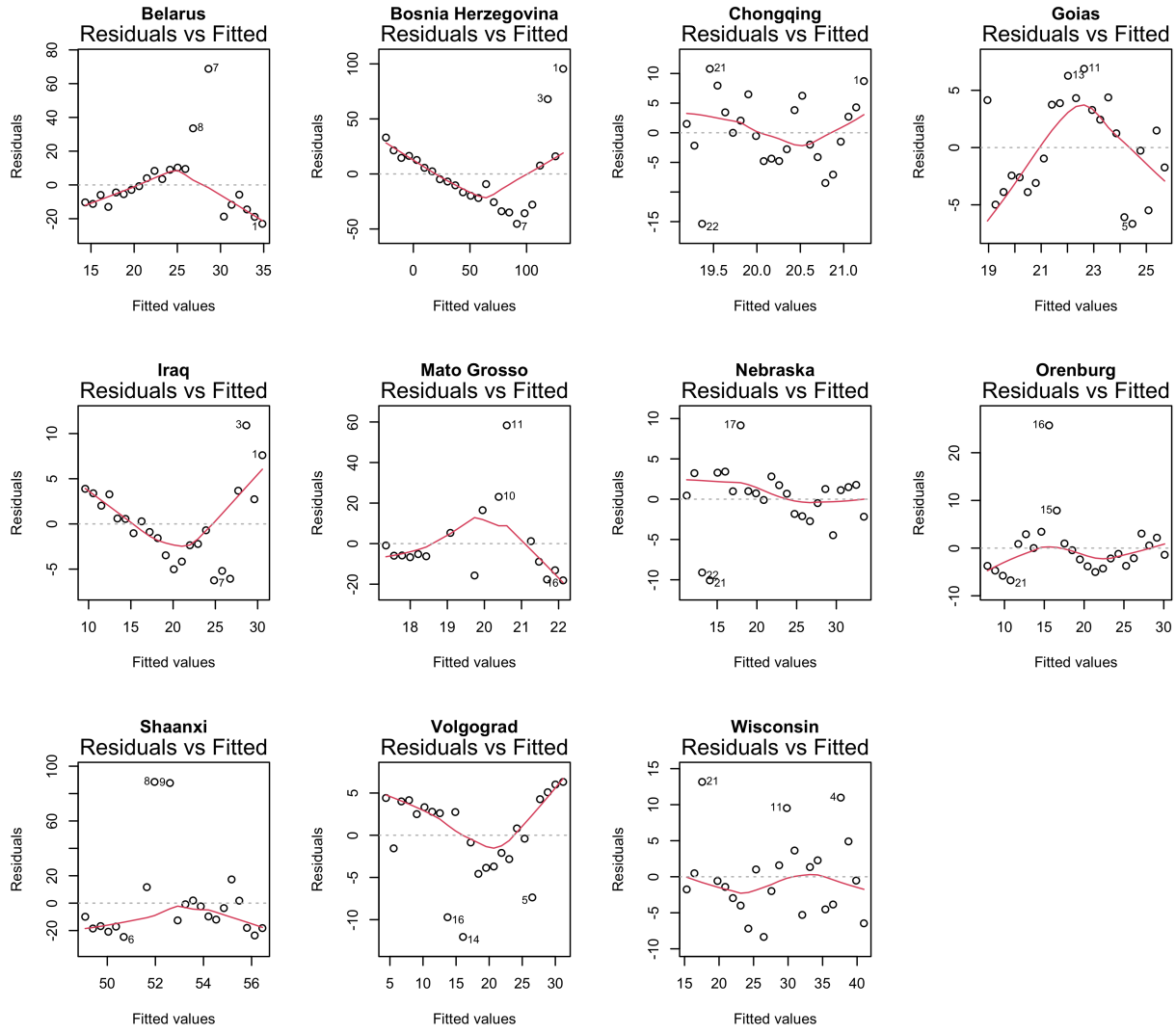


Figure S19: Residuals vs. fitted diagnostic plots for each site, for a simple `lm` call corresponding to Eq. (S3), in which the half-life (i.e., the time required for half (50%) of a given cohort of abandoned cropland to be recultivated) is modeled as a function of the year of initial abandonment at each site.

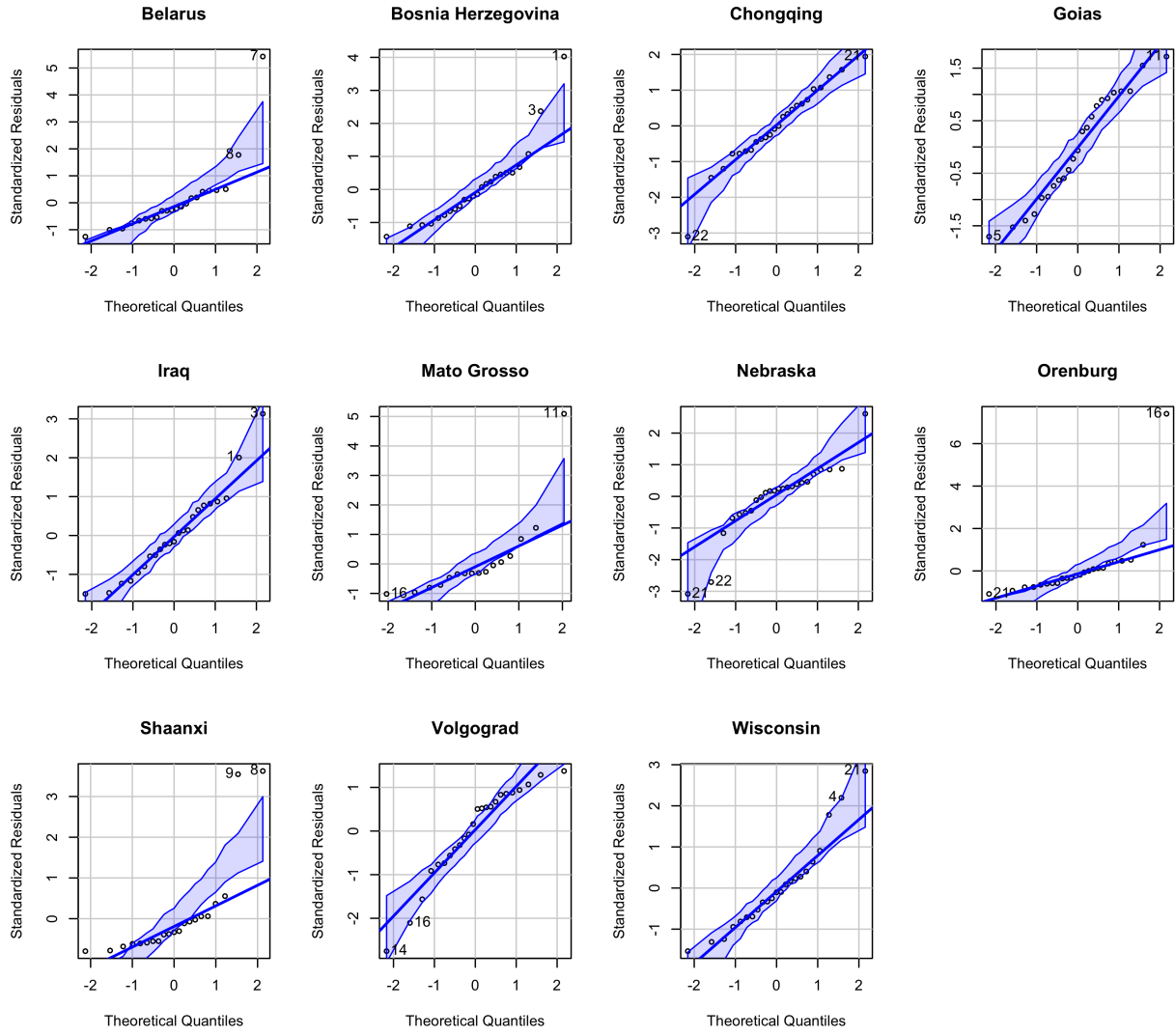


Figure S20: QQ plots calculated using the `car` package (14), for a simple `lm` call corresponding to Eq. (S3), in which the half-life (i.e., the time required for half (50%) of a given cohort of abandoned cropland to be recultivated) is modeled as a function of the year of initial abandonment at each site.

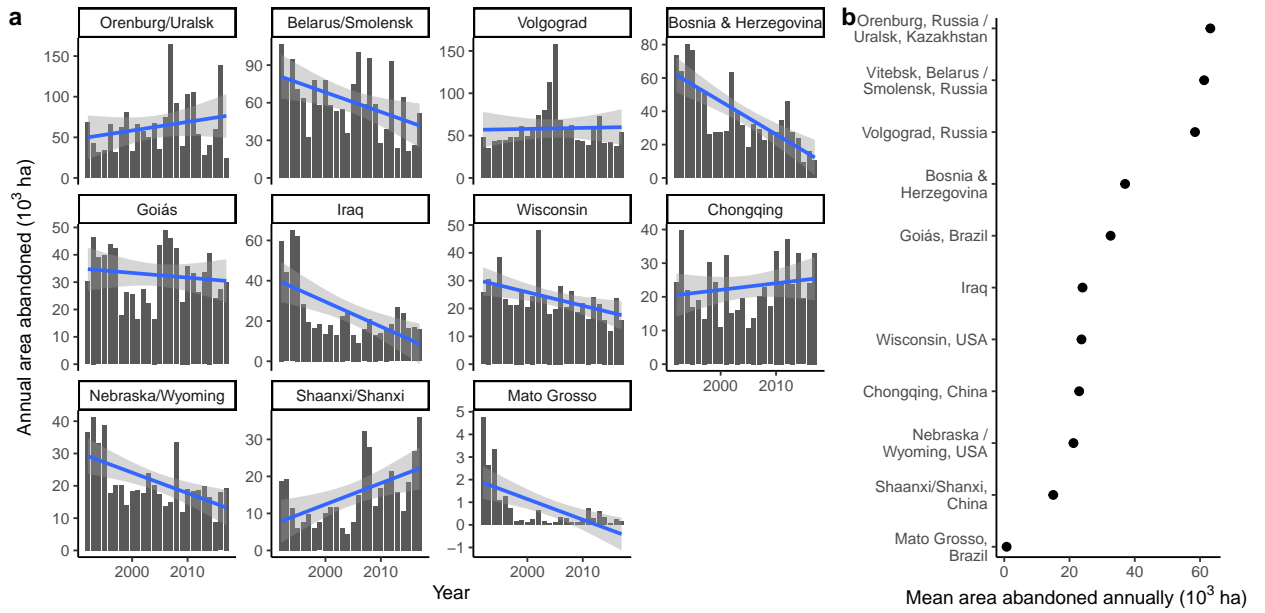


Figure S21: Annual gain in newly abandoned cropland at our eleven sites. Panel a shows the trend in annual abandonment over time at each site (in 10^3 ha), and Panel b shows the mean annual abandonment (in 10^3 ha) at each site. The mean values in panel b feed into the extrapolations. Note that the annual gain in abandonment corresponds to the dark green bars in Figure S5).

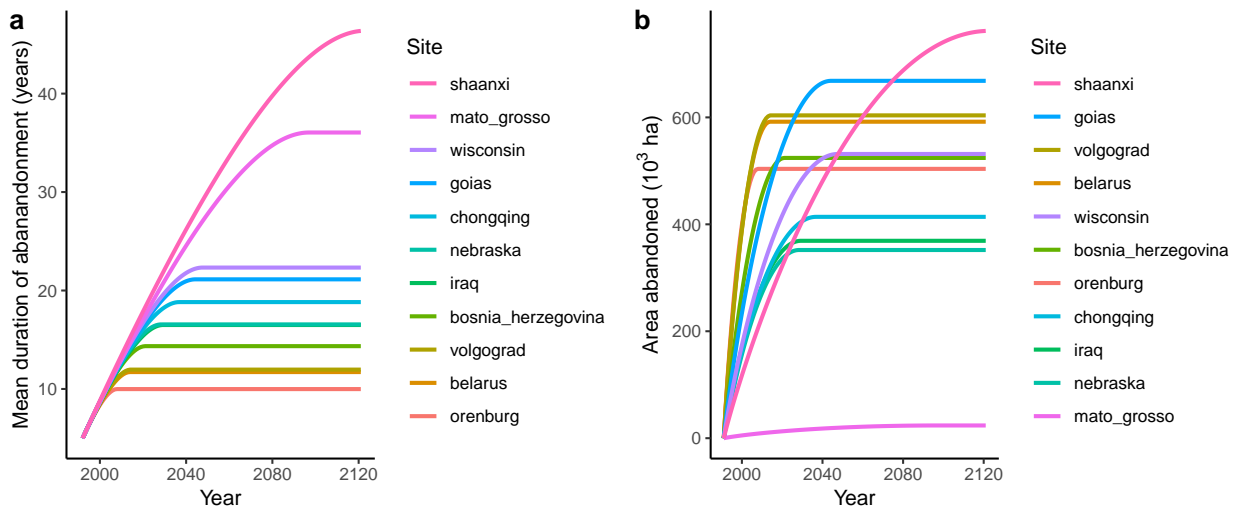


Figure S22: The results of our simple extrapolation, including a) the mean age of abandonment, and b) the total area abandoned into the future. Colors corresponding to each site are consistent across the three panels. These extrapolations assume recultivation based on the mean decay trend for each site Figure 3 and annual new abandonment based on the mean annual gain in abandonment shown in Figure S5 (dark green bars).

Extrapolation 1

Assuming i) mean decay rates and ii) constant area abandoned each year.

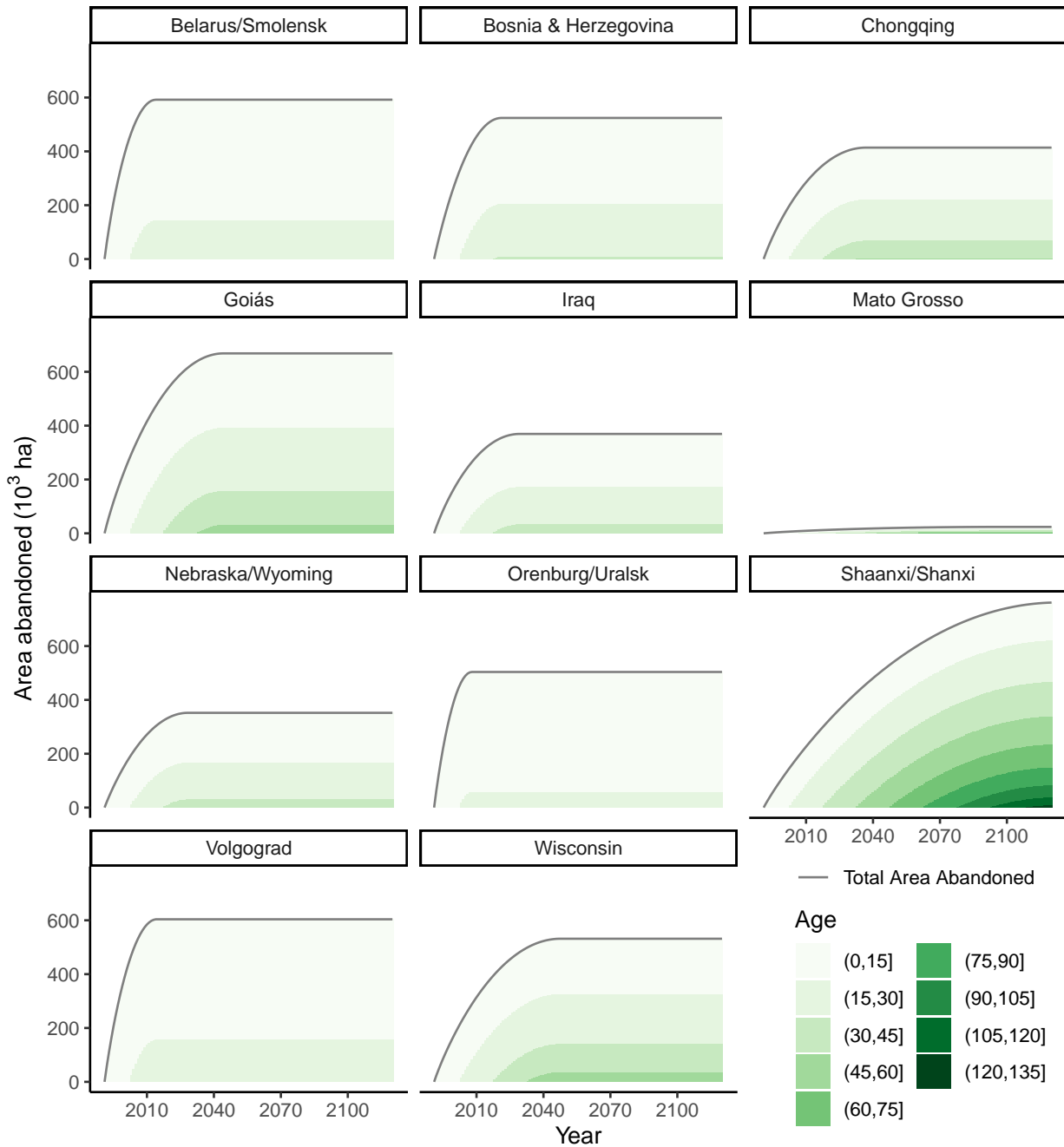


Figure S23: Extrapolating area by age bin, assuming a 1) each site follows the mean recultivation (“decay”) rate, and 2) a constant area abandoned each year (based on the mean annual area abandoned at each site).

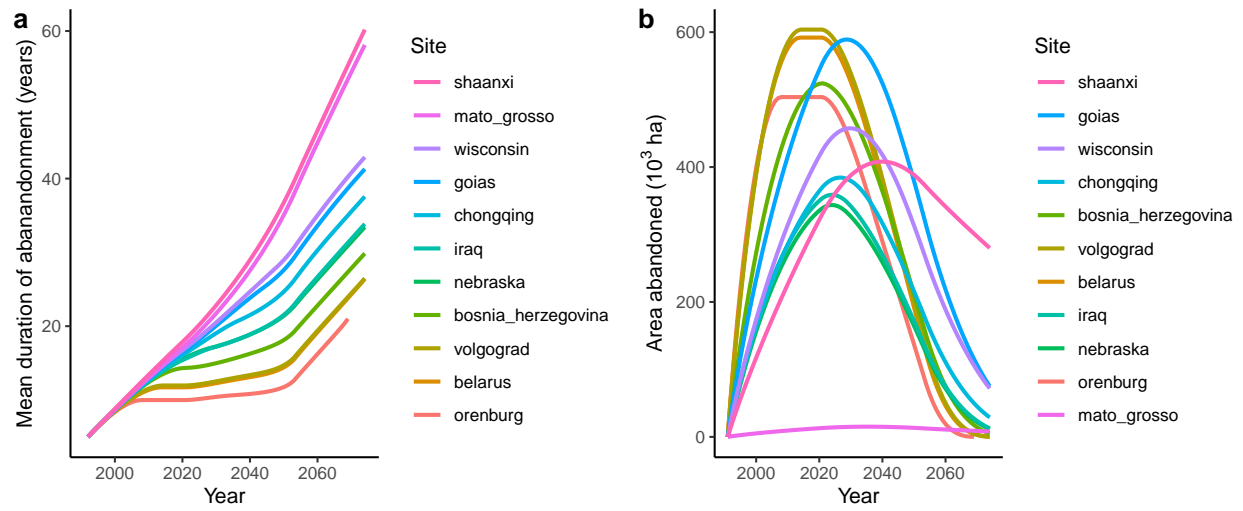


Figure S24: The results of our second extrapolation, including a) the mean age of abandonment, and b) the total area abandoned into the future. Colors corresponding to each site are consistent across the three panels. These extrapolations assume recultivation based on the mean decay trend for each site (Figure 3) and annual new abandonment based on the mean annual gain in abandonment shown in Figure S5 (dark green bars).

Extrapolation 2

Assuming i) mean decay rates and ii) constant area abandoned each year until 2017, then linear decline in area abandoned each year until reaching 0 in 2050.

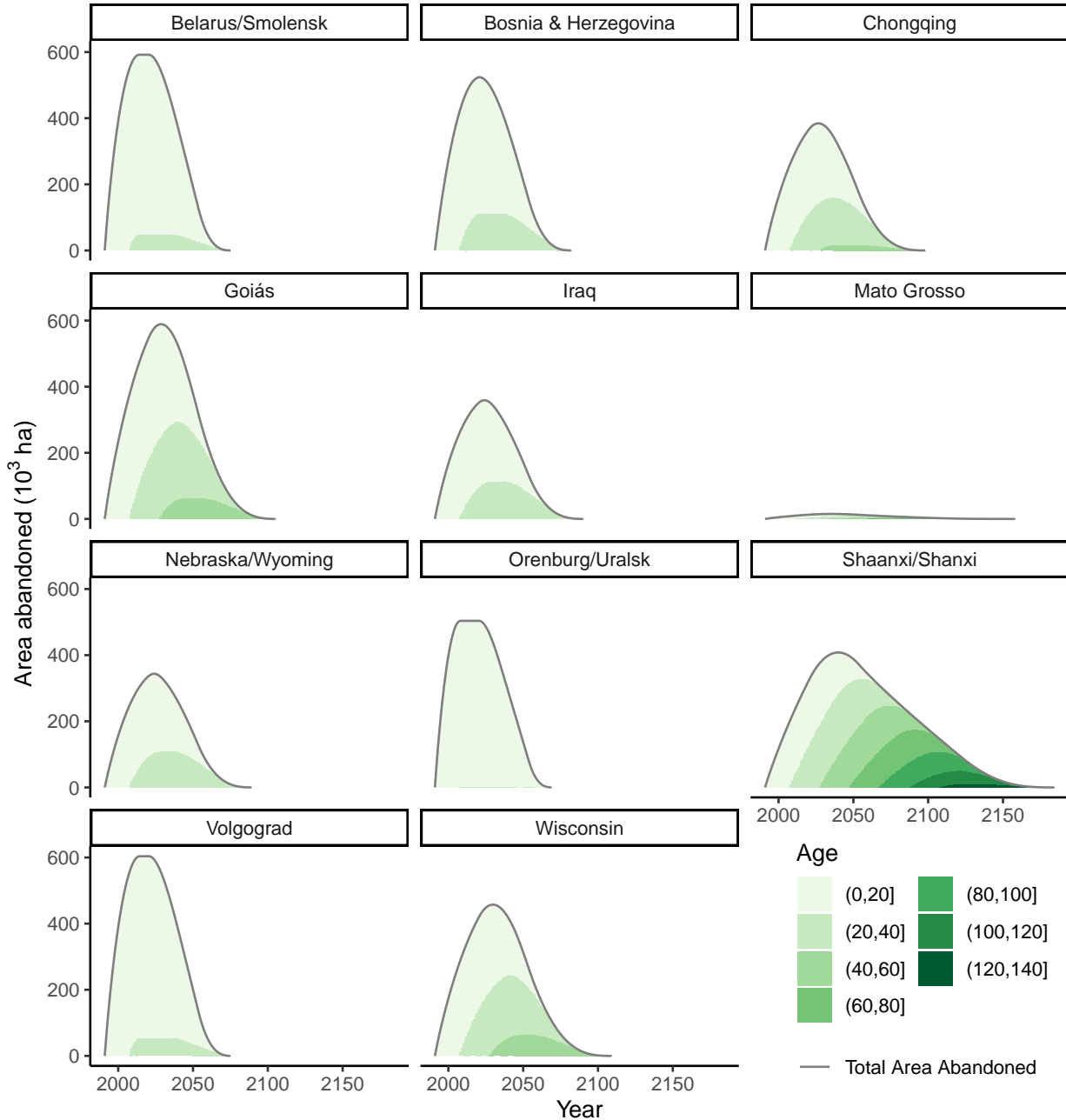


Figure S25: Extrapolating area by age bin, assuming a 1) each site follows the mean recultivation (“decay”) rate, and 2) a constant area abandoned each year until 2017 (based on the mean annual area abandoned at each site), followed by a linearly declining area abandoned each year until reaching 0 in 2050.

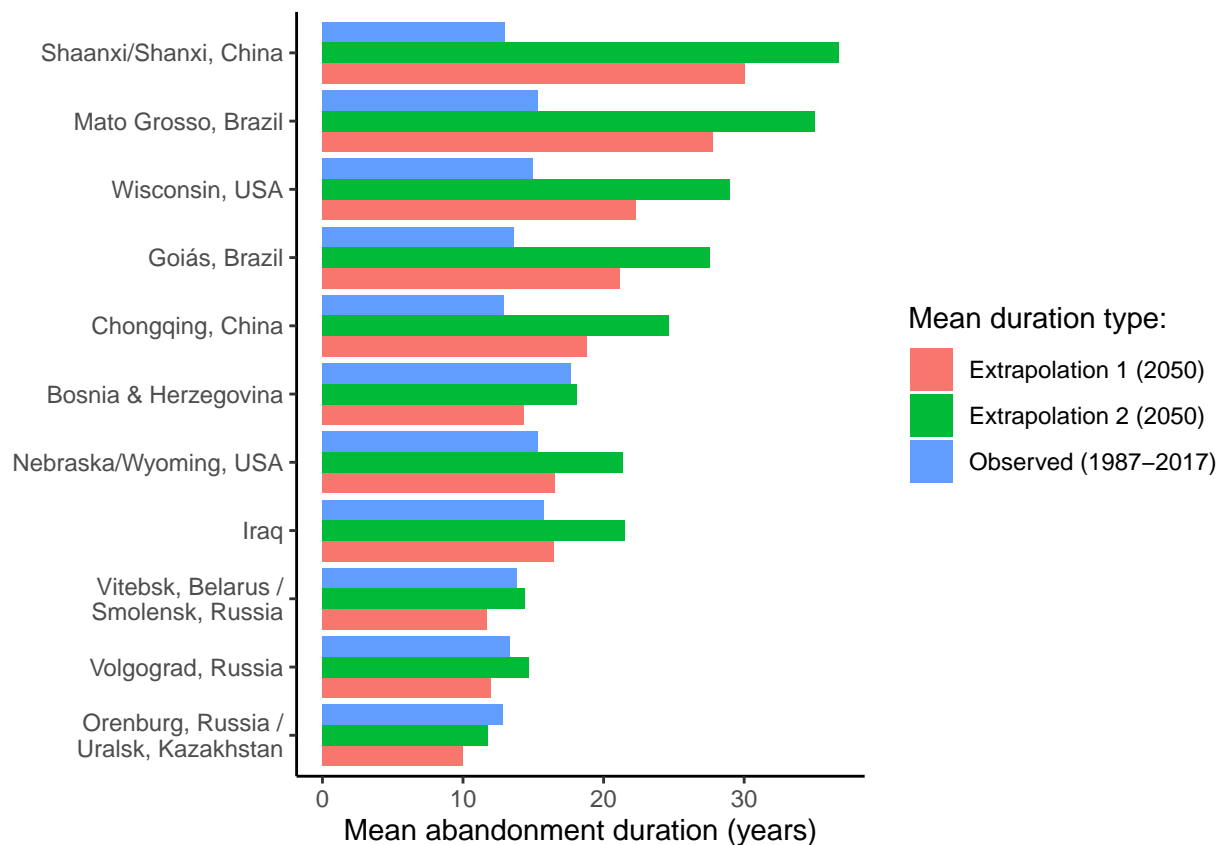


Figure S26: Comparing the mean duration of abandonment at our 11 sites observed between 1987 and 2017 with the extrapolated mean duration as of 2050 for our two extrapolations.

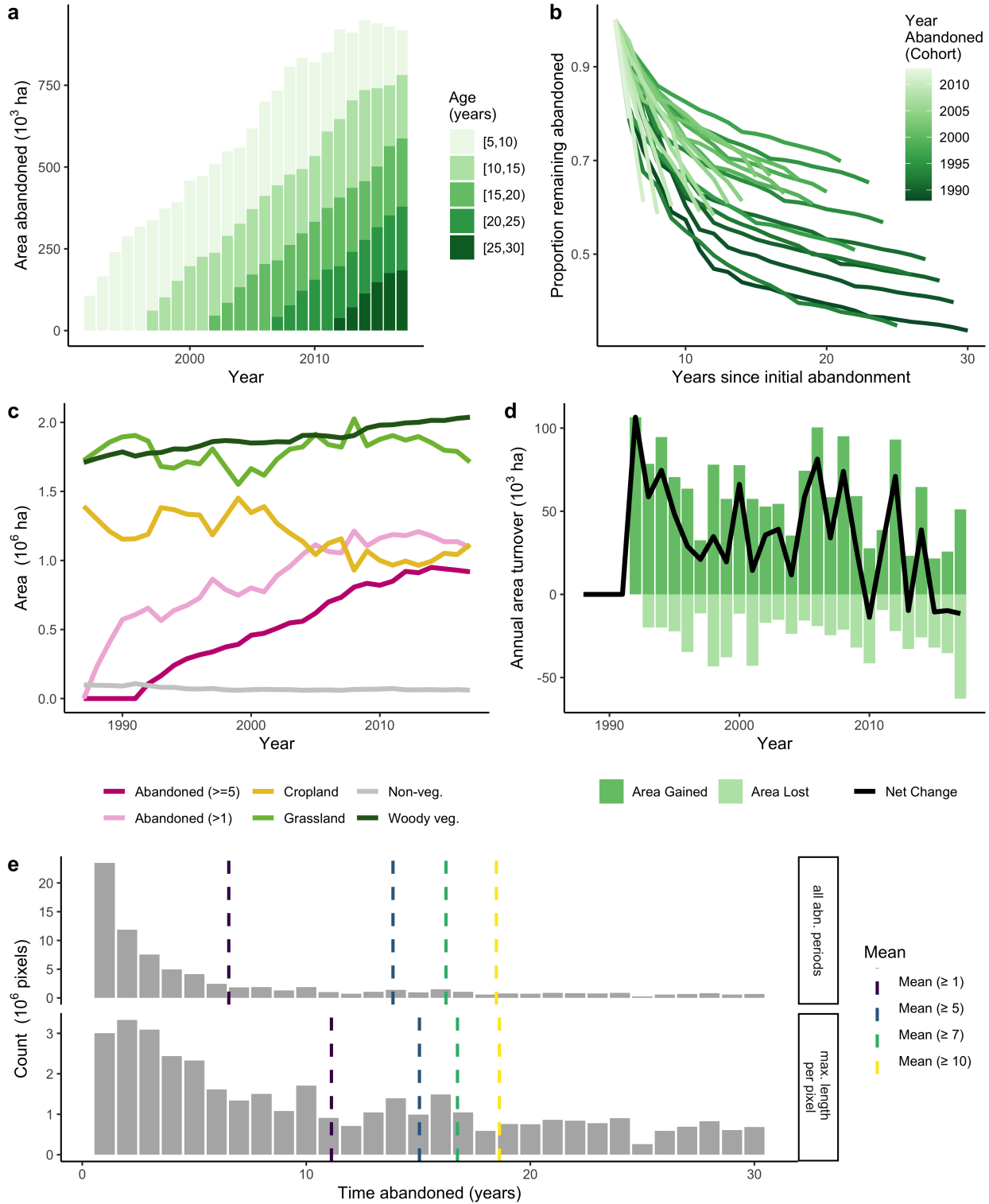


Figure S27: Abandonment patterns for Vitebsk, Belarus / Smolensk, Russia, showing a) accumulation of abandoned land by age class, b) decay of abandoned land by year abandoned, c) the area in each land cover class through time (including both land that has been abandoned for five or more years, as well as any land abandoned for 1 or more years, therefore including short-term fallows), d) the annual turnover of abandoned land through time, and e) the distribution of abandonment duration for all periods of cropland abandonment (top) and the maximum duration of abandonment at each pixel (bottom).

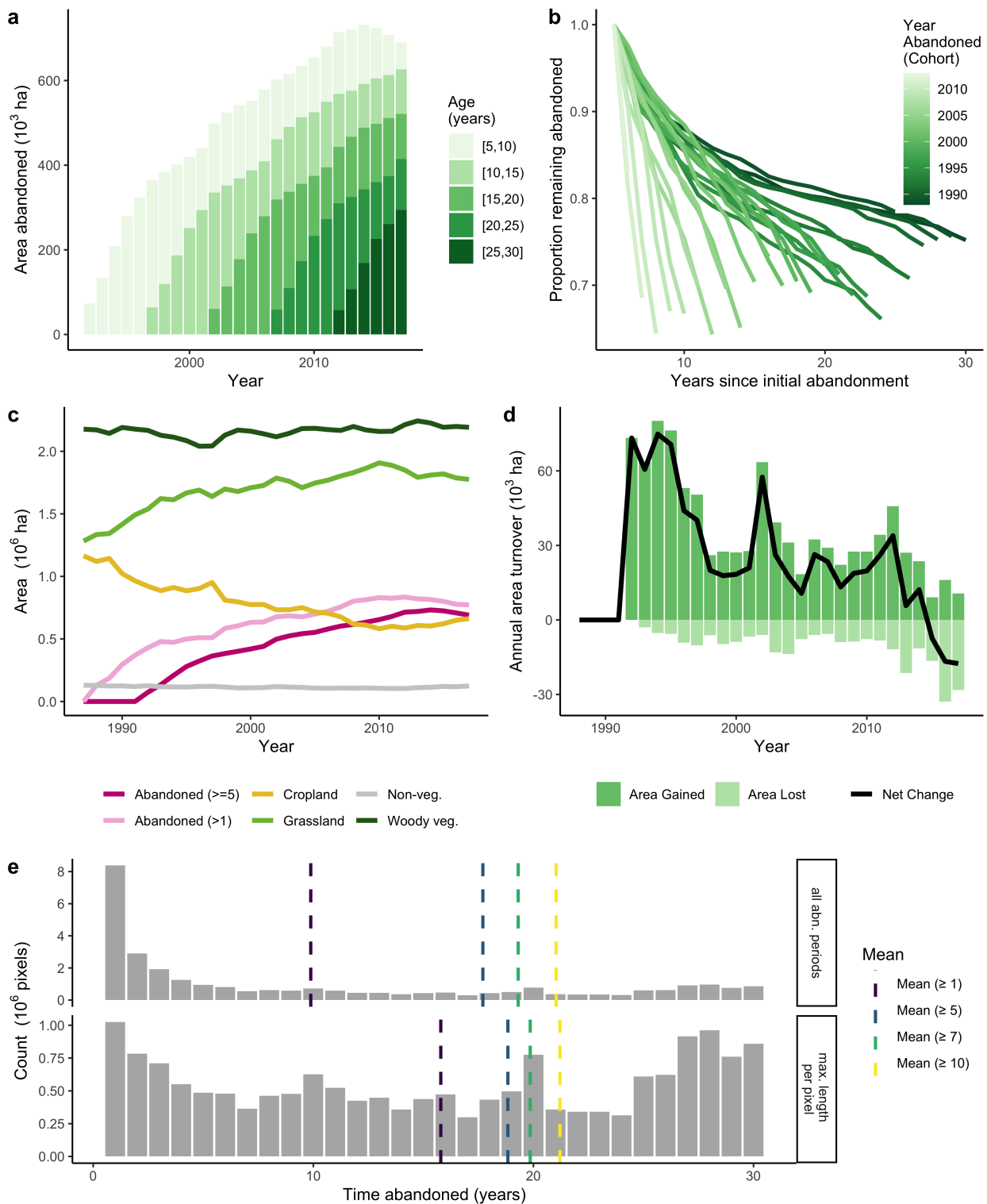


Figure S28: Abandonment patterns for Bosnia & Herzegovina, following Figure S27.

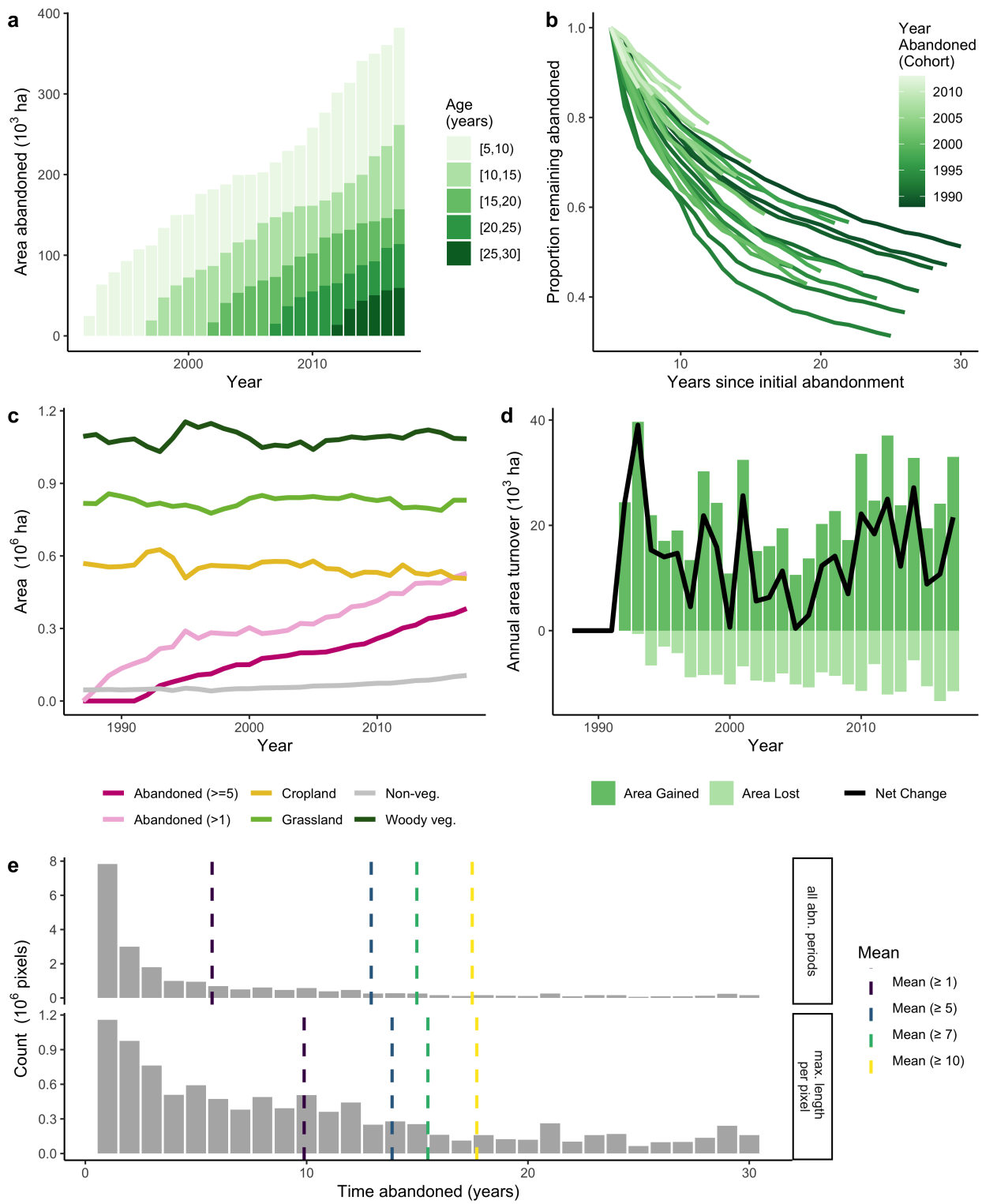


Figure S29: Abandonment patterns for Chongqing, China, following Figure S27.

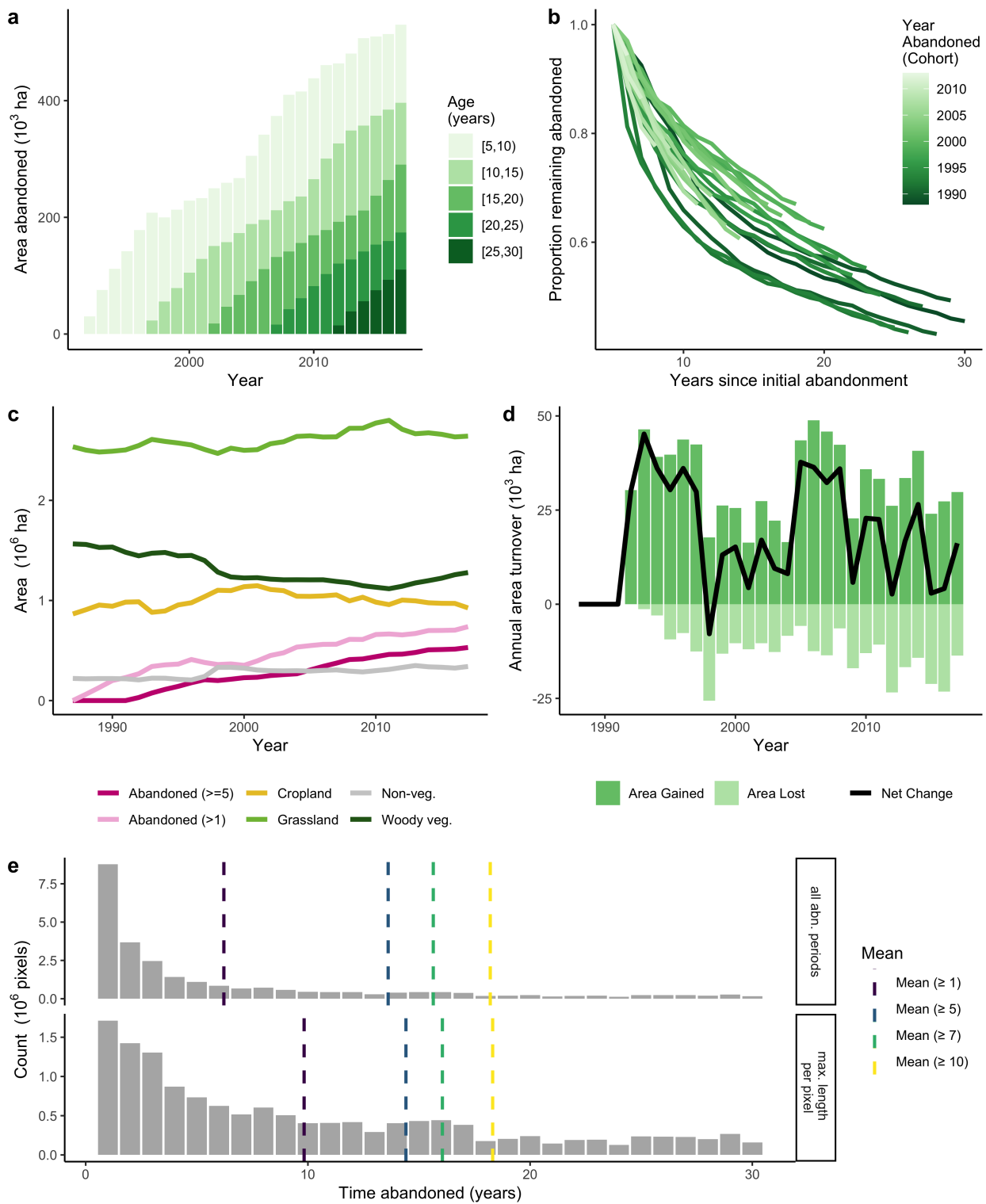


Figure S30: Abandonment patterns for Goiás, Brazil, following Figure S27.

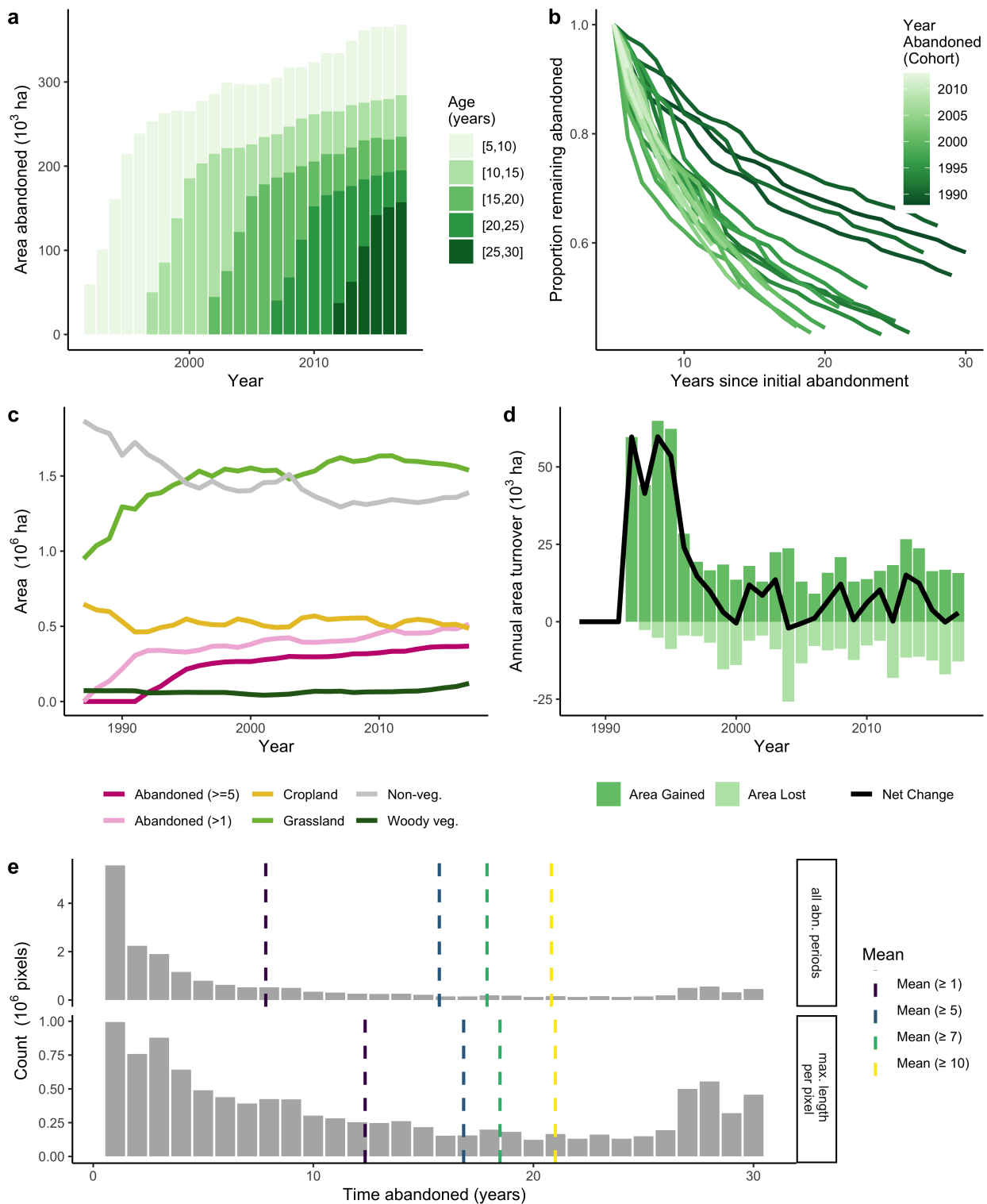


Figure S31: Abandonment patterns for Iraq, following Figure S27.

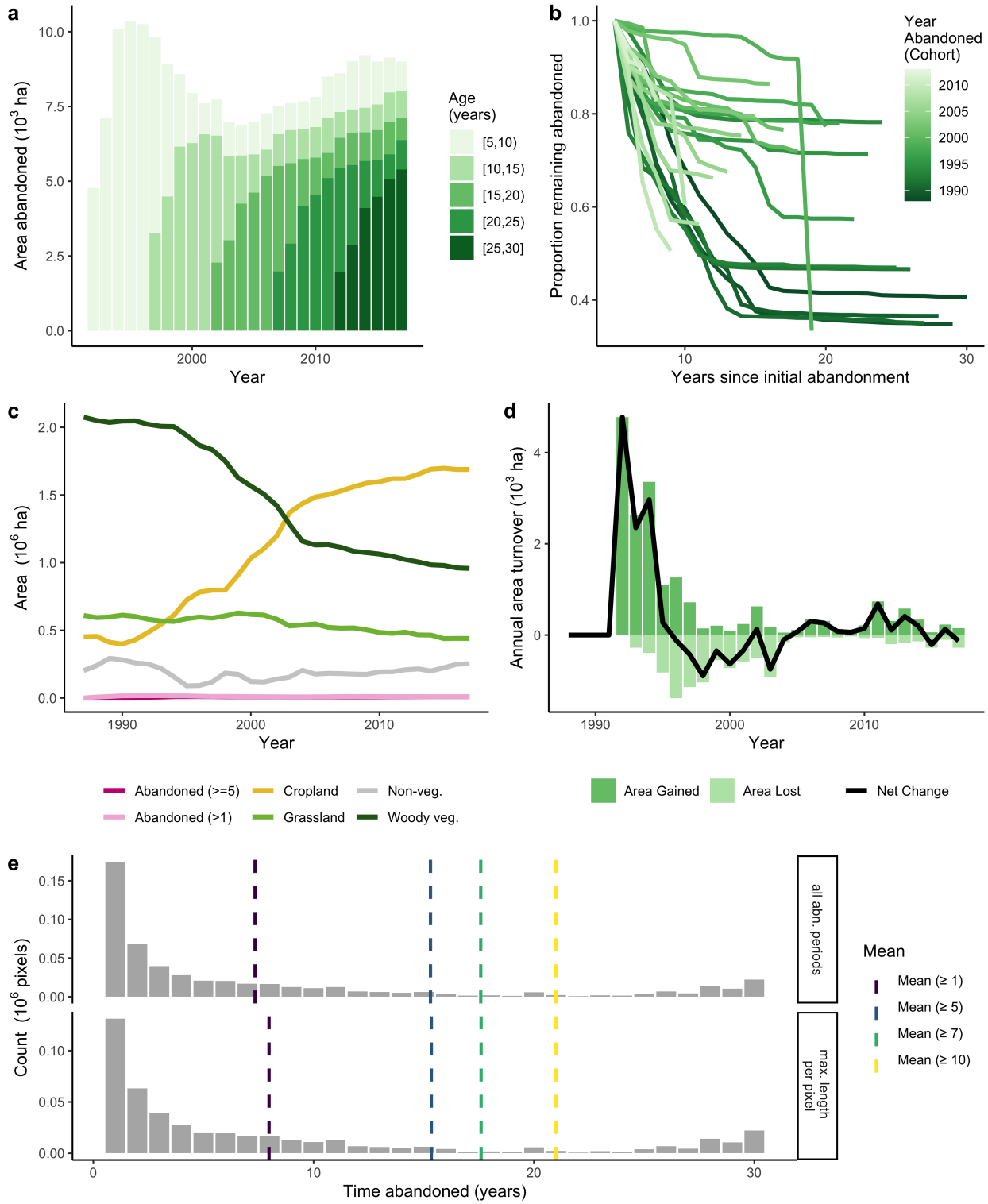


Figure S32: Abandonment patterns for Mato Grosso, Brazil, following Figure S27.

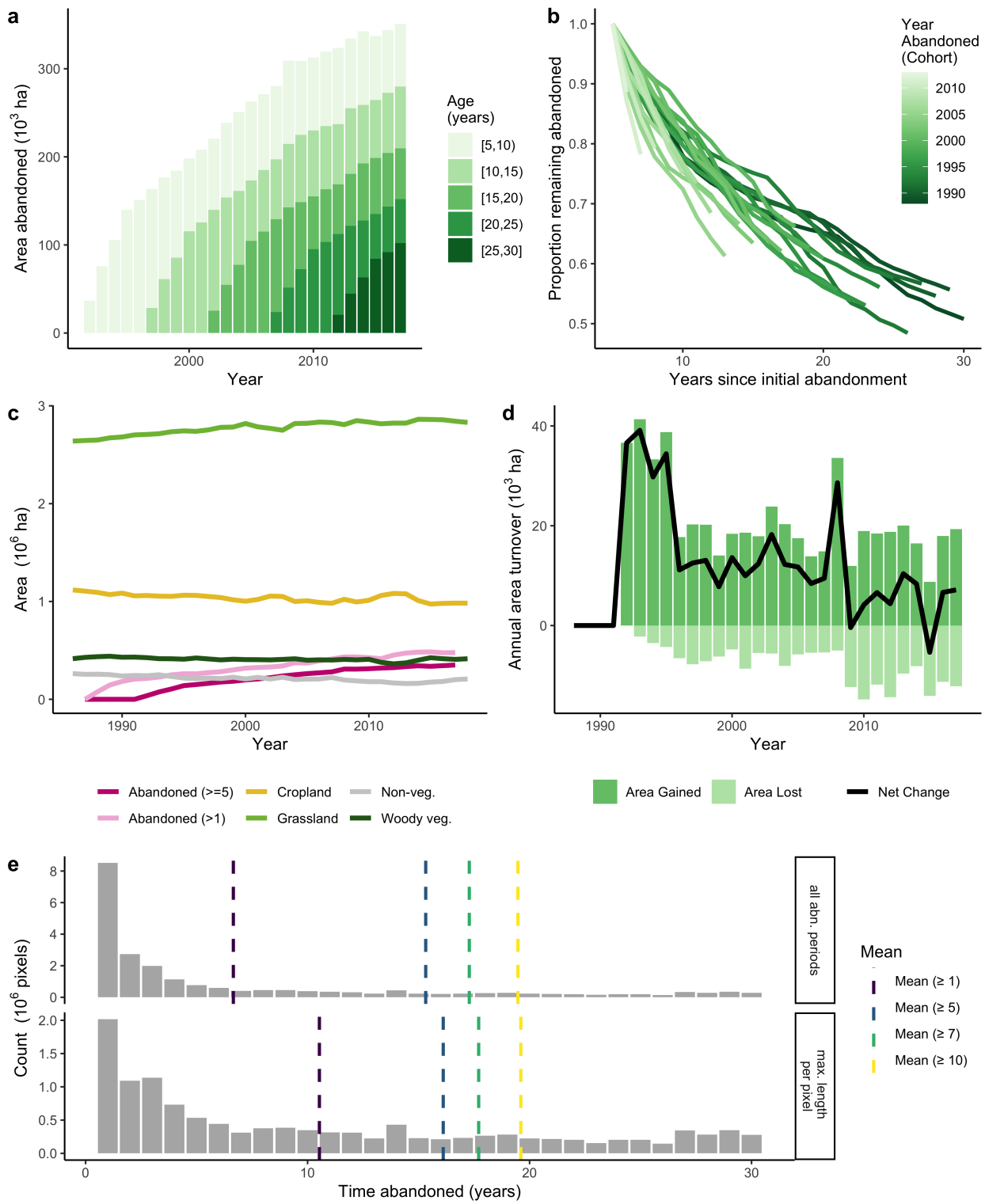


Figure S33: Abandonment patterns for Nebraska/Wyoming, USA, following Figure S27.

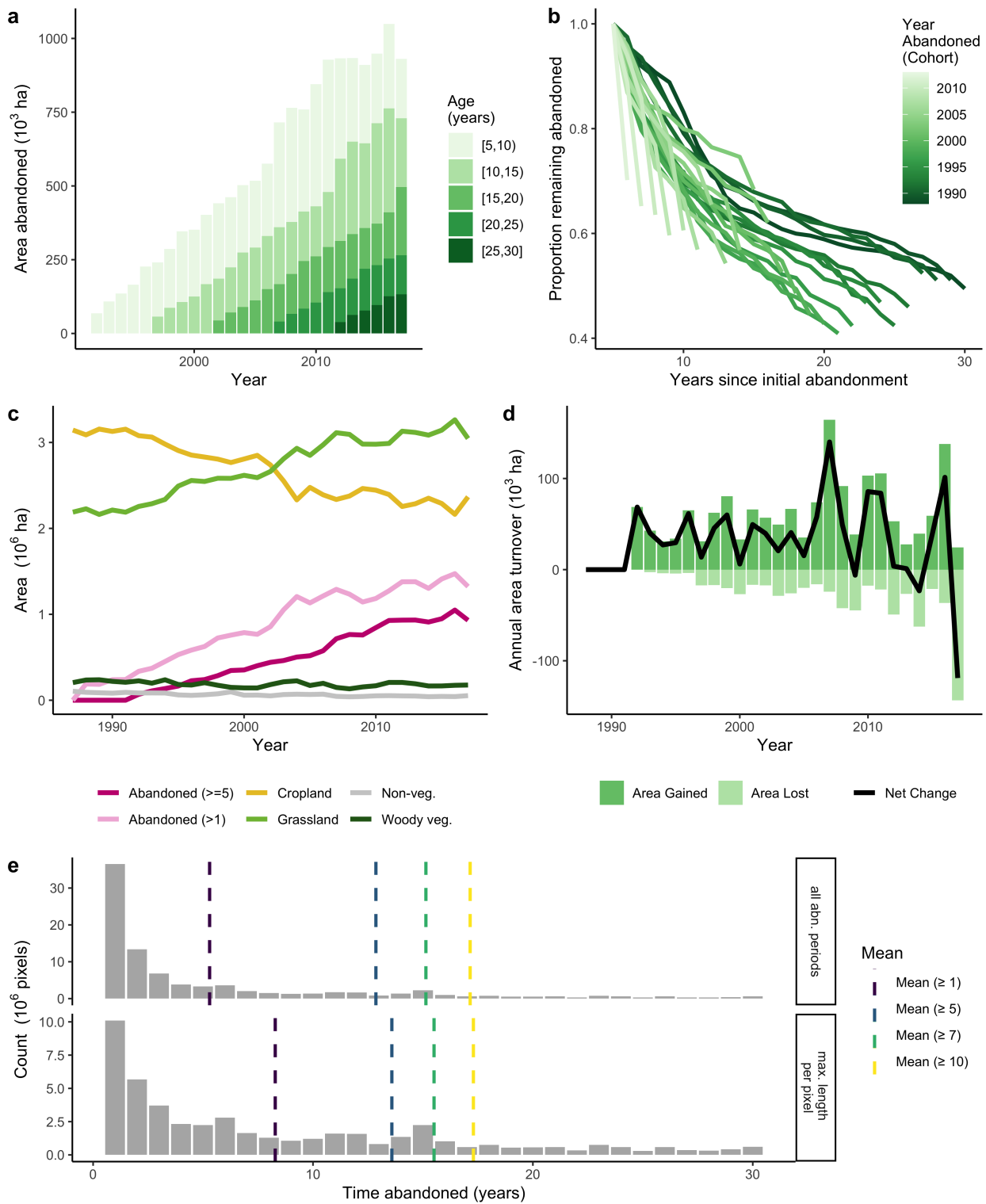


Figure S34: Abandonment patterns for Orenburg, Russia / Uralsk, Kazakhstan, following Figure S27.

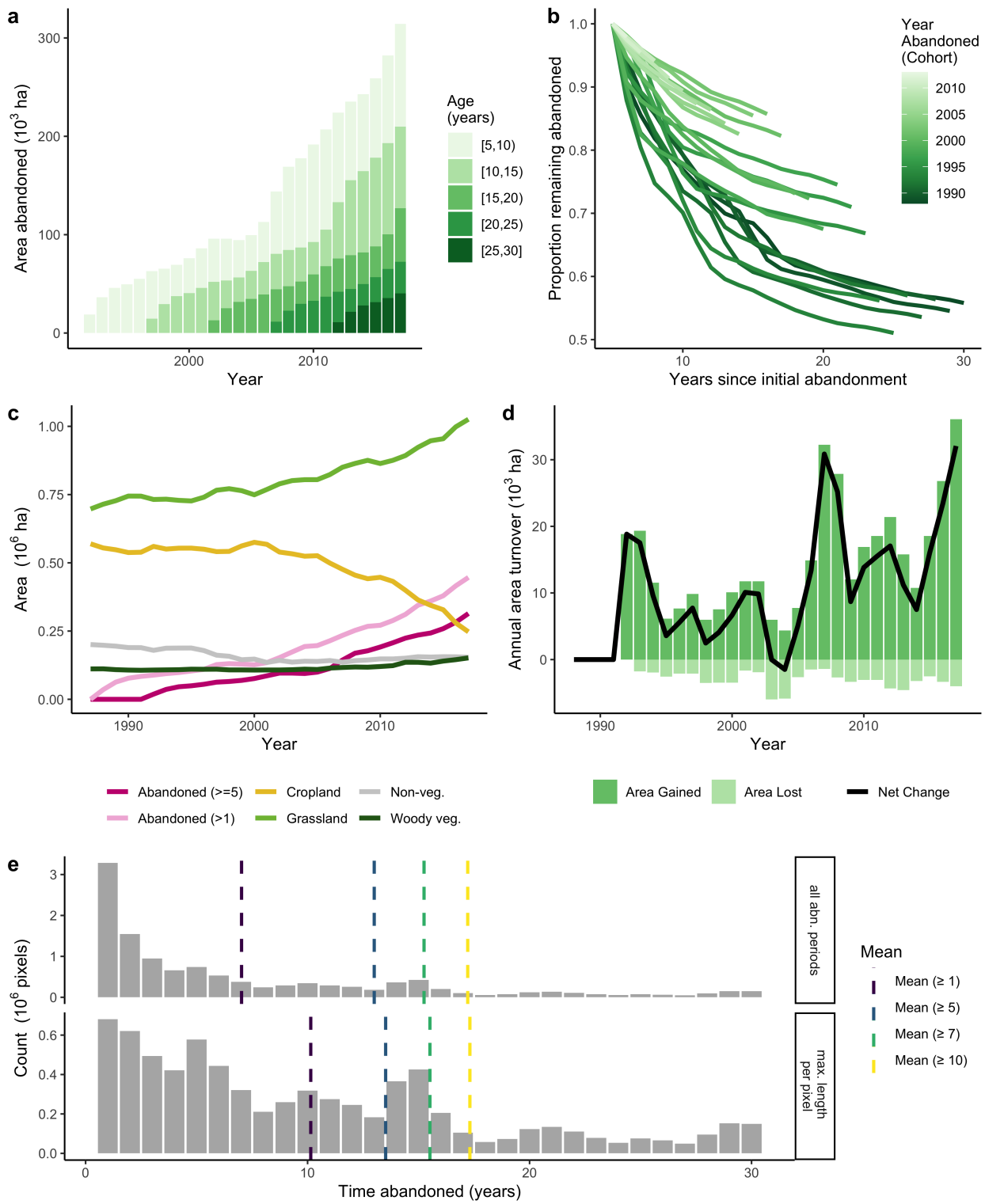


Figure S35: Abandonment patterns for Shaanxi/Shanxi, China, following Figure S27.

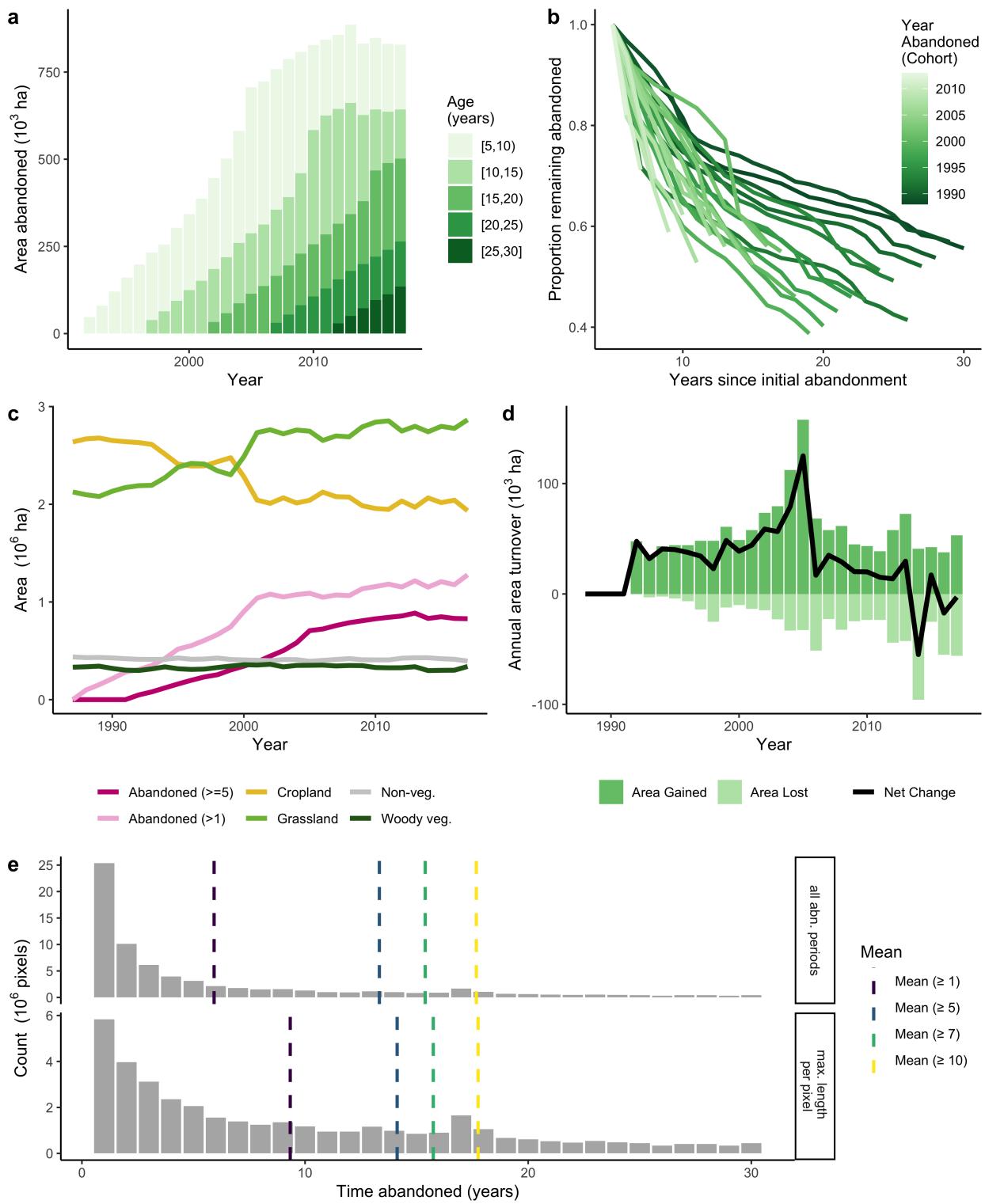


Figure S36: Abandonment patterns for Volgograd, Russia, following Figure S27.

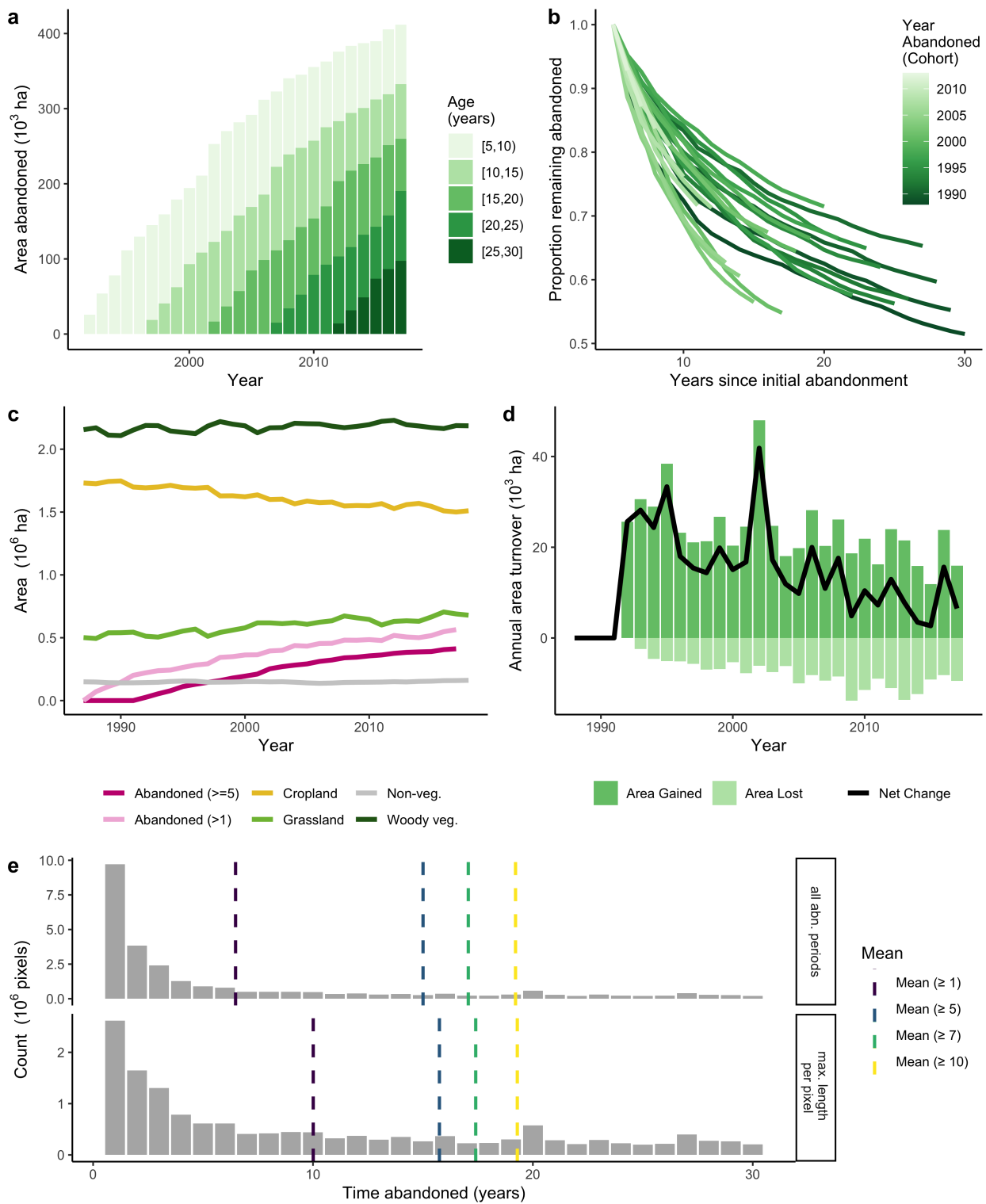


Figure S37: Abandonment patterns for Wisconsin, USA, following Figure S27.